NOLTR 62-65

UNRESOLVED FINE STRUCTURE OF THE NITRIC OXIDE GAMMA 0-0 BAND FOR THE DETERMINATION OF TEMPERATURE

18 JUNE 1962

NOL
UNITED STATES NAVAL ORDNANCE LABORATORY, WHITE OAK, MARYLAND

Ballistics Research Report 63

UNRESOLVED FINE STRUCTURE OF THE NITRIC OXIDE GAMMA 0-0 BAND FOR THE DETERMINATION OF TEMPERATURE

Prepared by:
David Levine

ABSTRACT: An experimental program was conducted to investigate the properties of the unresolved rotational fine structure of the nitric oxide γ_{00} band. The experimental values were taken spectroscopically in absorption at controlled temperatures.

An analytic expression representing the unresolved rotational fine structure is utilized to compute absorption coefficients and intensities of absorption for the experimental temperatures. A doublet model, a modified doublet model, and a singlet model of the band were investigated.

Experimental values for the intensity of absorption compared well with computed values from the doublet model over the band. Agreement also existed in the wings of the band when the singlet model was investigated.

From the experimental absorption coefficients, temperatures were determined to within 6 percent of the directly measured values. The rotational constants of the upper and lower states could be determined to 13 percent and 6 percent, respectively, of the known values.

U. S. NAVAL ORDNANCE LABORATORY
WHITE OAK, MARYLAND

UNRESOLVED FINE STRUCTURE OF THE NITRIC OXIDE GAMMA 0-0 BAND FOR THE DETERMINATION OF TEMPERATURE

This work was sponsored by the Special Projects Office of the Bureau of Naval Weapons, under the Applied Research Program in Aeroballistics.

The purpose of this investigation was to determine temperature by applying the properties of the unresolved spectra of a molecular band.

The author wishes to thank Dr. Theodore Marshall of this Laboratory and Dr. E. A. Mason of the University of Maryland for the advice rendered during the preparation of this work.

W. D. COLEMAN
Captain, USN
Commander

A. E. Seigel

A. E. SEIGEL
By direction

CONTENTS

ILLUSTRATIONS

TABLES

Section 1

INTRODUCTION

PURPOSE

The investigation was generated by a desire to examine spectroscopically molecular species occurring in a shocktube event. The shocktube is a powerful tool for obtaining conditions of pressure, density, and temperature over a wide range of values. However, analysis of the shocktube event is complicated by the short duration in which there is equilibrium of the internal degrees of freedom of a molecular gas. This duration is of the order of milliseconds. The coupling of spectroscopic techniques to the analysis of conditions in the shocktube is an excellent method for obtaining experimental values in spite of the limitations of the shocktube. The spectrograph is capable of recording information over the short duration of events, it is sensitive to extremely small concentrations of species, and even to those species which may exist only fleetingly.

A necessary requisite for the interpretation of experimental values obtained from a shocktube event is a knowledge of the temperature during the period when the internal degrees of freedom of the molecular gases are in equilibrium. To facilitate the measurement of temperature it was decided to examine the rotational fine structure of a molecular band. A choice of the molecule to be investigated would require its existence in the experimental environment and a knowledge of the molecular parameters. Because air is often used as the working gas in a shocktube, nitric oxide, which exists in some concentration in air at elevated temperatures, was chosen for this investigation.

Besides its existence, which is of prime importance, nitric oxide possesses other properties which are desirable for this specific investigation. The molecule is diatomic and the theory of the diatomic molecule is well established. The δ_{oo} band occurs at 2169.4 Å which is a region of high dispersion for the Bausch and Lomb medium quartz spectrograph used to obtain the experimental values. Also, the δ_{oo} band is strongly absorbing, allowing data to be taken using absorbing techniques. It was necessary that the experimental information be taken in absorption so that the temperature of the gas could be controlled and measured for each run. In absorption the property of interest is the absorption coefficient. The calculation of the absorption coefficient and of the emission intensity is similar. All theoretical considerations apply to both with only slight modifications. Since the experimental values were taken in absorption, calculations are made for the absorption coefficient and for the intensity of absorption.

ROTATIONAL FINE STRUCTURE OF A MOLECULAR BAND (ref. (1) and (2))

The structure of a molecule and its radiative process are similar to those of an atom. Both possess a positively charged core in which most of the mass is concentrated. Both possess orbital electrons which are arranged according to the Pauli exclusion principle. For both, a radiative event in which a discrete frequency is observed occurs when there is a change of stationary states resulting in the emission or absorption of energy. The principal difference between the atom and the molecule is that the atomic core is a single nucleus possessing only translational degrees of freedom. The molecular core is composed of two or more nuclei and possesses translational, vibrational and rotational degrees of freedom. The vibrational and rotational states of the molecule couple with, and modify the electronic states, giving rise to a spectrum more complicated than that of an atom. An atomic transition between two electronic states gives rise to one or several spectral lines depending on the multiplicities of the states. A molecular transition involving two electronic states gives rise to a "band" series. In addition, each band possesses a rotational fine structure, the result of coupling the rotational states to the electronic-vibrational states. It is this rotational fine structure which gives to the molecular bands their characteristic shape.

The energy associated with the emission or absorption of a discrete frequency may be approximately expressed as the sum of the electronic energy, the vibrational energy, and the rotational energy. Since this treatment deals only with the rotational fine structure of a single band of a band series, it is assumed that the electronic and vibrational energies are known. They will appear throughout this treatment as the terms which locate the origin of the particular band being discussed.

$$\frac{\Delta E_{electronic}}{hc} + \frac{\Delta E_{vibrational}}{hc} = \nu_0 \qquad (1)$$

The derivation of the rotational terms proceeds with the assumption that the diatomic molecule may be treated mathematically to a good approximation as a rigid rotor. A solution of the time-independent Schrodinger wave equation yields for the energy of the rigid rotor (ref. (3))

$$E = h^2 J(J+1)/(8\pi^2 I) = J(J+1)Bhc. \qquad (2)$$

J is the rotational quantum number, μ is the reduced mass of the molecule and r is the internuclear distance. B is termed the rotational constant and is inversely proportional to a moment of inertia. The rotational term becomes

$$F(J) = hJ(J+1)/(8\pi^2 c\mu r^2) = J(J+1)B. \qquad (3)$$

An analysis of the dipole transition for the rotational states yields the selection rules for the rotational quantum number J. They are $\Delta J = 0, \pm 1$ with the exceptions that $J' = 0 \longrightarrow J'' = 0$ does not occur and that $\Delta J = 0$ occurs only if at least one of the electronic states in the transition has a component of electronic angular momentum along the internuclear axis, Λ, greater than zero. From the term expressions, three equations are evolved, a consequence of the three transitions allowed by the selection rules. These are termed branch equations and are designated "P" for $\Delta J = -1$, "Q" for $\Delta J = 0$ and "R" for $\Delta J = 1$. Because the band origin is located by the electronic-vibrational terms, the location of each fine structure line relative to ν_0 is given by the three branch equations.

$$\nu_P = \nu_0 + F'(J-1) - F''(J), \qquad (4a)$$

$$\nu_Q = \nu_0 + F'(J) - F''(J), \qquad (4b)$$

$$\nu_R = \nu_0 + F'(J+1) - F''(J). \qquad (4c)$$

Primed terms designate the upper state of the transition and double primes the lower state. It is well to note that for a given molecule, the rotational constant B is different for each electronic state, and further modified by each vibrational state coupled to the electronic state. Therefore, rotational constants for the upper and lower states of a transition differ.

In general, the form of the branch equations is

$$\nu - \nu_0 = \alpha + \beta J + \gamma J^2, \qquad (5)$$

where α, β and γ represent combinations of the rotational constants. Mathematically the equations represent parabolas.

A plot of the branch equations for a molecule is called a Fortrat diagram. Such a diagram, for the nitric oxide γ_{00} band, is given in figure II.

If for some value of the rotational quantum number J a branch equation has a turning point, the branch is said to form a band head. The head is characterized by a sharp rise in intensity on one side and a gradual decrease of intensity on the other side. The direction of the degradation of intensity is a function of the rotational constants. If B' is greater than B'' the direction is to higher wave numbers, if B'' is greater than B' the direction is to lower wave numbers. All the branches of a molecular band depend on the same rotational constants and consequently are degraded in the same direction.

Generally, the features of the majority of molecular bands are one or several distinctive band heads described by the turning of a branch equation, a band origin which indicates the position of the forbidden transition $J' = 0 \longrightarrow J'' = 0$, and a degradation of intensities in a particular direction. The region of degradation will be referred to as the band wings.

ABSORPTION COEFFICIENT FOR ROTATIONAL FINE STRUCTURE (ref. (1))

The absorption coefficient for a given rotational fine structure transition is a function of the occupation of the initial state undergoing the transition and the probability that such a transition will occur. The occupation of the initial state is given by the Boltzmann distribution law and the probability by the Einstein transition probability for absorption.

For a thin optical layer, Δ X, one may write for the intensity of absorption

$$I_{abs.} = \rho_{nm} N_m B_{mn} h c \nu_{nm} \Delta X, \tag{6a}$$

where Nm is the number of molecules per cm^3 in the initial state, Bmn is the Einstein transition probability, $hc\nu$nm is the energy of a light quantum of wave number ν_{nm} and ρ_{nm} is the density of radiation of wave number ν_{nm}. I_0, the incident radiation intensity, is equal to the density of radiation multiplied by the velocity of light C. Equation (6a) becomes

$$I_{abs} = I_0 N_m B_{mn} h \nu_{nm} \Delta X. \tag{6b}$$

Nm may be expressed in terms of the Boltzmann factor. The sum over-all states, or the partition function Q, the total number of absorbing molecules, and the statistical weight for the state, 2J + 1.

$$N_m = [N(2J''+1)/Q]\, e^{-E/kT} = [N(2J''+1)/Q]\exp(-J''(J''+1)B''hc/kT). \quad (7)$$

k is the Boltzmann constant and T is the absolute temperature. The Einstein transition probability for absorption for a degenerate state is given by

$$B_{mn} = (8\pi^3/3h^2c)\,\Sigma_i (|R^{n_i, m_i}|)^2/(2J''+1). \quad (8)$$

R^{nm} is the matrix element for the electric dipole moment. If one substitutes equations (7) and (8) in equation (6b) the resulting equation is

$$I_{abs} = I_0 \frac{N}{Q}\frac{8\pi^3}{3hc}\nu_{nm}\exp(-J''(J''+1)B''hc/kT)\,\Sigma_i (|R^{n_i, m_i}|)^2 \Delta X$$

$$= I_0 A \Delta X. \quad (9)$$

A is called the absorption coefficient. For the general case of the finite absorbing layer the equation for the intensity of absorption is

$$I_{abs.} = I_0 (1 - e^{-AX}). \quad (10)$$

To consider intensity of emission the occupation of the excited state Nn and the Einstein transition coefficient for emission would be substituted. I_0 and ΔX would not enter into the equation.

It is well to consider at this point the validity of equation (9). The derivation does not take into account occupation or transition probability of the electronic state. Equation (9) is correct for absolute values of the absorption coefficient for vibrational transitions if one also takes into account induced emission. Such transitions occur in the infrared. For the rotational fine structure of an electronic transition the

relation is useful only in normalized form to give relative intensities. It is with a modified form of the normalized equation that this study deals.

UNRESOLVABILITY OF ROTATIONAL FINE STRUCTURE AND THE ENVELOPE OF INTENSITY (ref. (4))

By use of the branch equations and the equations for absorption or emission intensity, it is possible to locate a rotational transition and assign to it a relative intensity. Knowledge of the rotational constants and the absolute temperature is necessary for this procedure. Conversely, if rotational transitions can be resolved, rotational constants and temperatures can be determined. However, the limitations placed on the recording of data in a shocktube necessitate the use of a spectrograph with a large optical aperture. Such instruments generally are not capable of resolving the rotational fine structure of a molecular band. Even under conditions of very high resolution rotational components cannot be resolved when the term differences are smaller than the line breadths. This condition exists for most molecules in the region of band heads and in regions extending well into the wings for molecules which are formed by the overlapping of many branches. In the shocktube conditions are worsened by the degree of line broadening caused by conditions of pressure and temperature. The problem then is to obtain from the unresolved rotational fine structure of a molecular band, a method for measuring temperature and possibly obtaining the rotational constants. Previous work with unresolved fine structure (ref. (5)) has been limited to the determination of temperature by the painstaking averaging of rotational intensities to obtain an intensity envelope.

An alternate procedure would be to obtain an analytic expression for the envelope of intensities. Conceivably, both the temperature and the rotational constants could then be obtained. The derivation of such an analytic expression requires a criterion for unresolvability. This criterion is that adjacent rotational lines of a branch depending on quantum numbers J-1, J and J + 1 cannot be resolved. Therefore, the three transitions may be represented by a single parametric quantum number m. The expression for the absorption coefficient now determines a value over a region $\delta\nu$. Dividing by an expression for the density of states in the region $\delta\nu$, one obtains an expression for the absorption coefficient as a function of the parametric quantum number m. The relation for the density of states is obtained by differentiating the branch equation with respect to $\Delta\nu$. The equation in normalized form for the absorption coefficient becomes

$$A = \frac{S \exp(-m^2 B^2 hc/kT)}{B + 2mB} \qquad (11)$$

The term S is the line strength and is that part of $\sum (|R^{m,m-1}|)^2$ which depends on the rotational quantum number.

The equations in the form (11) require the calculation of intensities for each branch of the band. It is possible to solve the branch equations for the rotational quantum number in terms of $\Delta\nu$. $\Delta\nu$ is here taken with respect to the initial head of the band rather than with respect to the origin. The absorption coefficient is then given as a single equation as a function of $\Delta\nu$ band head.

Equations in the general form of equation (11) were computed to yield the absorption coefficient for several different models of the nitric oxide γ_{00} band. Curves are presented for the intensity of absorption for several different temperatures and compared with experimental results.

Section 2

EXPERIMENTAL PROCEDURE

The experimental apparatus consisted of a Bausch and Lomb medium quartz spectrograph, an absorption cell, and a source of continuous radiation.

The absorption cell was fabricated of vycor with fused silica windows. It was 30.5 cm. in length and 2.54-in. in diameter. The cell was filled with commercial nitric oxide supplied by the Matheson Corporation. The nitric oxide is 98 percent pure. The method of filling the cell was to draw a vacuum of several tenths of a millimeter of mercury and then to fill it with nitric oxide to atmospheric pressure. The process was repeated a number of times and then the cell was finally filled to 15 millimeters of nitric oxide and permanently sealed. The effective absorbing path of the gas was 0.6 cm.

The source of continuous radiation was a hydrogen discharge tube obtained from the Hanovia Corporation. The discharge tube was watercooled and powered by a transformer which supplied an operating voltage of approximately 2,000 volts to the discharge tube. The intensity of the discharge tube was kept constant over the duration of the experiment by regulating the line voltage.

The four experimental temperatures were obtained by placing the absorption cell in a cylindrical oven 13 inches in length. The oven was open at both ends and consisted of a helical heating element surrounded by insulating material. Initial temperature measurements in the oven showed a large temperature gradient from the center to the ends. A heavy-walled brass pipe was inserted in the oven to smooth the gradient. The use of the brass pipe reduced the gradient to the order of 2°C.

The absorption cell was inserted in the oven and the ends were sealed with fiberglas batting, allowing only the central portions of the entrance and exit windows of the absorption cell to be exposed. The temperature of the oven was controlled with a variac and monitored with a copper-constantan thermocouple. The thermocouple was constructed to give the average temperature over the length of the absorption cell by having 13 junctions spaced at one-inch intervals and connected in parallel and placed along the length of the absorption cell. No concerted effort was made to calibrate the thermocouple. The steam point was measured and found to be less than one-degree centigrade below 100°C. Values for the thermocouple emf vs temperature for the entire experiment were obtained from the National Bureau of Standards Tables. A conservative estimate of the accuracy of the temperature measurements is better than plus or minus 5°C. The deviations indicated in the experimental temperatures tabulated in Table I are average deviations from the mean value. Temperatures were recorded every minute during each exposure.

The Bausch and Lomb medium quartz spectrograph had a dispersion over the nitric oxide γ_{oo} band of 5Å per millimeter with a variation of less than one percent. The resolution of the instrument in this region is 0.3Å or approximately 6 wave numbers. The effective aperture of the spectrograph is f24. The cover lens has a focal length of 50 cm. The hydrogen source was placed at the focal point of the cover lens with the absorption cell immediately in front of the source. The slit height used for recording the data was 5 millimeters, which was smaller than the diameter of the source. Slit widths of 40, 20 and 10 microns were used, with the majority of runs taken at 20 microns. The light which passed through the absorption cell and illuminated the spectrograph slit was effectively parallel.

The spectrograms were recorded on Eastman type IVf spectrographic plates. The emulsion was sensitized for ultraviolet by coating with ultraviolet sensitizer #2 supplied by Distillation Products Industry. The sensitizer was dissolved in cyclohexane and applied before exposure to the emulsion. Before development, the sensitizer was removed by washing in cyclohexane. The plate

was then developed for two minutes in D 19. During the two-minute development period the plate was continuously brushed to minimize development defects. The fixing and washing procedures were standard.

The emulsion was calibrated by taking seven exposures of the constant hydrogen light source ranging from 15 seconds to 16 minutes in a geometric progression. Long calibration exposures and data exposures were used to minimize timing errors. The relatively insensitive type IV f plates were well suited for the long exposures. Calibration data were reduced on a microdensitometer and calibration curves were obtained for each 2 Å sector over the range of the band. Seven calibration curves were used to obtain significant information from the experimental values.

Exposures for all 20-micron slit width runs were taken at 16-minute exposures. The single 10-micron and 40-micron exposures were taken at 32-minute and 8-minute exposure times, respectively.

Although some 30 plates were exposed during the course of the investigation, the final values were obtained from a single plate. With calibration, the results presented were obtained from two spectrographic plates.

Section 3

REDUCTION OF EXPERIMENTAL INFORMATION

The photographic images were reduced to density traces by scanning the spectrograms with a recording microdensitometer. The instrument used was a Knorr-Albers recording microdensitometer manufactured by Leeds and Northrup. Spectrograms were scanned at one millimeter per minute. The strip chart recorder travel was 2 inches per minute, giving an apparent dispersion of 2.5 Å per inch for the density traces. Values were recorded every 0.1 Å in the regions where intensity variations were large. In the regions of the band where intensity was slowly varying, values were taken every 0.25 Å. Information taken directly from the densitometer charts was reduced to significant intensity values by the use of the calibration curves for the emulsion described in the preceding section.

To compensate for the effects of the slit function, exposures were taken at 40-micron and 10-micron slit widths at a temperature of 296°K. The slit function has the effect of reducing the observed intensity of absorption in the region

where the intensity of absorption is rapidly varying. The 40-micron and 10-micron slit width data were used to extrapolate the 20-micron slit data to zero slit width. This procedure was necessary because a mathematical correction for the slit function can be made only for a spectral line whose shape is attributed to Doppler broadening, collision broadening, or a combination of the two. Because no such mathematical shape can be assigned to an integrated intensity of absorption, the procedure outlined appears to be the only method for making the corrections.

The intensities of absorption for the 6 runs are tabulated in Tables II through VII. The intensity of absorption values given in the tables have their origin in the various times used for the calibration exposure. In the final presentation, values are normalized and are dimensionless.

Section 4

THE NITRIC OXIDE γ_{00} BAND

THE DOUBLET MODEL (ref. (1), (2), (6), (7), and (8))

The γ series for the nitric oxide molecule is the result of a transition between doublet terms. The upper state of the transition is a $^2\Sigma$ which has an electron angular momentum component along the internuclear axis, Λ, equal to zero. The ground state of the transition is a $^2\pi_{1/2,3/2}$ which has Λ equal to one.

The $^2\Sigma$ state belongs to Hund's coupling case (b). (ref. (1) and (2)). For this case, Λ and S, the resultant electron spin, are not coupled and no doublet splitting occurs. A quantum number K is defined which is the total angular momentum apart from spin and takes values

$$K = \Lambda, \Lambda+1, \Lambda+2 \ldots\ldots \tag{12}$$

The resultant J is given by

$$J = (K+S), (K+S-1), \ldots\ldots |K-S|. \tag{13}$$

The $^2\pi_{1/2,3/2}$ state belongs to Hund's coupling case (a). (ref. (1) and (2)) For this case, Λ and S are coupled and the doublet splitting occurs. A quantum number Ω is now defined as the sum of Λ and S and the resultant J is given by

$$J = \Omega, \Omega+1, \Omega+2, \cdots \tag{14}$$

For the $^2\Sigma \longrightarrow {}^2\Pi_{1/2,3/2}$ transition, one obtains 12 branches. The term values which give rise to the branches are for the $^2\Sigma$ state

$$\begin{aligned} F_1'(J) &= B'k(k+1) = B'(J-1/2)(J+1/2) \\ F_2'(J) &= B'k(k+1) = B'(J+1/2)(J+3/2), \end{aligned} \tag{15a}$$

and for the $^2\Pi_{1/2,3/2}$ state

$$\begin{aligned} F_1'' &= B_{eff}^{(1)} J(J+1) \\ F_2'' &= B_{eff}^{(2)} J(J+1) \end{aligned} \tag{15b}$$

The values for the rotational constants were obtained from the literature. B_{eff} is the rotational constant of the $^2\Pi_{1/2,3/2}$ state modified by the doublet splitting and is given by

$$B_{eff} = B''\left(1 \pm \frac{B''}{A_0 A} \cdots\right). \tag{16}$$

A_0 is the doublet splitting equal to 124 Cm^{-1}. The values of the constants for the γ_{00} band of nitric oxide are B' = 1.9870 Cm^{-1}, $B_{eff}^{(1)}$ = 1.6370 Cm^{-1}, and $B_{eff}^{(2)}$ = 1.7189 Cm^{-1}. The expressions for the 12 branches are

$$P_1 \qquad \nu = \nu_0^{(1)} + 3/4\,B' - (2B' + B_{eff}^{(1)})J + (B' - B_{eff}^{(1)})J^2 \tag{17a}$$

$$R_1 \qquad \nu = \nu_0^{(1)} + 3/4\,B' + (2B' - B_{eff}^{(1)})J + (B' - B_{eff}^{(1)})J^2 \tag{17b}$$

$$Q_1 \qquad \nu = \nu_0^{(1)} - 1/4\,B' - B_{eff}^{(1)}J + (B' - B_{eff}^{(1)})J^2 \tag{17c}$$

$$P_2 \qquad \nu = \nu_0^{(1)} - 1/4\,B' - B_{eff}^{(1)}J + (B' - B_{eff}^{(1)})J^2 \tag{17d}$$

$$R_2 \qquad \nu = \nu_0^{(1)} + 15/4\,B' + (4B' - B_{eff}^{(1)})J + (B' - B_{eff}^{(1)})J^2 \tag{17e}$$

$$Q_{21} \qquad \nu = \nu_0^{(1)} + 3/4 B' + (2B' - B_{44}^{(1)})J + (B' - B_{44}^{(1)})J^2, \tag{17f}$$

$$R_2 \qquad \nu = \nu_0^{(2)} - 1/4 B' - B_{44}^{(2)} J + (B' - B_{44}^{(2)}) J^2, \tag{17g}$$

$$R_2 \qquad \nu = \nu_0^{(2)} + 15/4 B' + (4B' - B_{44}^{2}) J + (B' - B_{44}^{(2)}) J^2, \tag{17h}$$

$$Q_2 \qquad \nu = \nu_0^{(2)} + 3/4 B' + (2B' - B_{44}^{(2)}) J + (B' - B_{44}^{(2)}) J^2, \tag{17i}$$

$$P_{12} \qquad \nu = \nu_0^{(2)} + 3/4 B' - (2B' - B_{44}^{(2)}) J + (B' - B_{44}^{(2)}) J^2, \tag{17j}$$

$$R_{12} \qquad \nu = \nu_0^{(1)} + 3/4 B' + (2B' - B_{44}^{(1)}) J + (B' - B_{44}^{(2)}) J^2, \tag{17k}$$

$$Q_{12} \qquad \nu = \nu_0^{(2)} - 1/4 B' - B_{44}^{(2)} J + (B' - B_{44}^{(2)}) J^2. \tag{17l}$$

The nitric oxide γ_{00} band is a double-headed double-band system. The head-forming branches are P_{12}, P_2, Q_{12}, P_1, Q_1, and P_{21}. The band is generally classified as an eight-branch system because there is a superposition of bands (R_1, Q_{21}) of (Q_1, P_{21}), of (P_2, Q_{12}), and of (Q_2, R_{12}). This is readily seen by examination of the branch equations. If all that were required of the spectroscopic data was evaluation of the rotational constants, and equipment was available to resolve the fine structure, then no attention need be paid to the superimposed branches. However, for the case of unresolved rotational fine structure, the absorption coefficient must be computed and the contribution of all the branches is necessary. Each branch of the band is represented by a different expression for the line strength. In effect, the line strength indicates the probability that a transition will occur. The line strengths (ref. (9)) for the $^2\Sigma \rightarrow {}^2\Pi_{1/2,3/2}$ transition are given both in terms of J, and in modified form for m, the parametric rotational quantum for unresolved fine structure.

$$S_{J'} = 1/32J \left\{ [2J+1]^2 + \frac{[2J+1][(2J+1)^2 - 2\lambda]}{[(2J+1)^2 - 4\lambda + \lambda^2]^{1/2}} \right\} \approx m/8 + 1/16 \frac{(4m^2 - 2\lambda)}{(4m^2 - 4\lambda + \lambda^2)^{1/2}} \tag{18a}$$

$$S_{R_1} = \frac{1}{32(J+1)}\left\{[2J+1]^2 + \frac{[2J+1][(2J+1)^2-8+2\lambda]}{[(2J+1)^2-4\lambda+\lambda^2]^{1/2}}\right\} \approx m/8 + \frac{1}{16}\frac{(4m^2-8+2\lambda)}{(4m^2-4\lambda+\lambda^2)^{1/2}} \quad (18b)$$

$$S_{Q_1} = \frac{(2J+1)}{32J(J+1)}\left\{[2J+1]^2 + 2 + \frac{[(2J+1)^3-8J-8+2\lambda]}{[(2J+1)^2-4\lambda+\lambda^2]^{1/2}}\right\} \approx m/4 + \frac{1}{8m} + \frac{(4m^3-4m-4-\lambda)}{8m(4m^2-4\lambda+\lambda^2)^{1/2}} \quad (18c)$$

$$S_{P_{21}} = \frac{1}{32J}\left\{[2J+1]^2 - \frac{[2J+1][(2J+1)^2-8+2\lambda]}{[(2J+1)^2-4\lambda+\lambda^2]^{1/2}}\right\} \approx m/8 - \frac{1}{16}\frac{(4m^2-8+2\lambda)}{(4m^2-4\lambda+\lambda^2)^{1/2}} \quad (18d)$$

$$S_{R_{21}} = \frac{1}{32(J+1)}\left\{[2J+1]^2 - \frac{[2J+1][(2J+1)-2\lambda]}{[(2J+1)^2-4\lambda+\lambda^2]^{1/2}}\right\} \approx m/8 - \frac{1}{16}\frac{(4m^2-2\lambda)}{(4m^2-4\lambda+\lambda^2)^{1/2}} \quad (18e)$$

$$S_{Q_{21}} = \frac{(2J+1)}{32J(J+1)}\left\{[2J+1]^2 + 2 - \frac{[(2J+1)^3-8J+2\lambda]}{[(2J+1)^2-4\lambda+\lambda^2]^{1/2}}\right\} \approx m/4 + \frac{1}{8m} - \frac{(4m^3-4m-\lambda)}{8m(4m^2-4\lambda+\lambda^2)^{1/2}} \quad (18f)$$

$$S_{P_2} = \frac{1}{32J}\left\{[2J+1]^2 + \frac{[2J+1][(2J+1)^2-8+2\lambda]}{[(2J+1)^2-4\lambda+\lambda^2]^{1/2}}\right\} \approx m/8 + \frac{1}{16}\frac{(4m^2-8+2\lambda)}{(4m^2-4\lambda+\lambda^2)^{1/2}} \quad (18g)$$

$$S_{R_2} = \frac{1}{32(J+1)}\left\{[2J+1]^2 + \frac{[2J+1][(2J+1)^2-2\lambda]}{[(2J+1)^2-4\lambda+\lambda^2]^{1/2}}\right\} \approx m/8 + \frac{1}{16}\frac{(4m^2-2\lambda)}{(4m^2-4\lambda+\lambda^2)^{1/2}} \quad (18h)$$

$$S_{Q_2} = \frac{(2J+1)}{32J(J+1)}\left\{[2J+1]^2 + 2 + \frac{[(2J+1)^3-8J-2\lambda]}{[(2J+1)^2-4\lambda+\lambda^2]^{1/2}}\right\} \approx m/4 + \frac{1}{8m} + \frac{(4m^3-4m-\lambda)}{8m(4m^2-4\lambda+\lambda^2)} \quad (18i)$$

$$S_{P_{12}} = \frac{1}{32J}\left\{[2J+1]^2 - \frac{[2J+1][(2J+1)^2-2\lambda]}{[(2J+1)^2-4\lambda+\lambda^2]^{1/2}}\right\} \approx m/8 - \frac{1}{16}\frac{(4m^2-2\lambda)}{(4m^2-4\lambda+\lambda^2)^{1/2}} \quad (18j)$$

$$S_{R_{12}} = \frac{1}{32(J+1)}\left\{[2J+1]^2 - \frac{[2J+1][(2J+1)^2-8+2\lambda]}{[(2J+1)^2-4\lambda+\lambda^2]^{1/2}}\right\} \approx m/8 - \frac{1}{16}\frac{(4m^2-8+2\lambda)}{(4m^2-4\lambda+\lambda^2)^{1/2}} \quad (18k)$$

$$S_{Q_{12}} = \frac{(2J+1)}{32J(J+1)}\left\{[2J+1]^2 + 2 - \frac{[(2J+1)^3-8J-8+2\lambda]}{[(2J+1)^2-4\lambda+\lambda^2]^{1/2}}\right\} \approx m/4 + \frac{1}{8m} - \frac{(4m^3-4m-4-\lambda)}{8m(4m^2-4\lambda+\lambda^2)^{1/2}} \quad (18l)$$

λ is the splitting constant for the band and for nitric oxide is taken to be 73. λ is equal to A_e/B''.

If equations (15a) through (15l) are examined, it is seen that for small values of λ, one has essentially a six-branch system consisting of the P_1, Q_1, R_1, P_2, Q_2, and R_2 branches. In effect one now approaches a singlet-like structure for the band with (P_1, P_2), (R_1, R_2), and (Q_1, Q_2), very nearly superimposed. This type of transition falls under the classification of Hund's case (b) previously discussed.

If λ is allowed to become very large, a system of 12 branches exists in which P and R branches are very nearly equal and Q branches are approximately twice the value of the P or R branches. This second transition belongs to Hund's case (a).

In reality the nitric oxide γ band series is transitional between Hund's cases (a) and (b). This relative position of the series, with respect to possible extremes of the doublet constant, causes the calculation of absorption coefficient to become somewhat involved.

If the band belonged to Hund's case (b) which is specified by the relation (ref. (2))

$$0 \leq \lambda \leq 4, \tag{19}$$

the line strengths could be approximated for the P_1, P_2, R_1 and R_2 branches by m/4, and for the Q_1 and Q_2 branches by m/2. The P_{12}, R_{12}, Q_{12}, P_{21}, R_{21}, and Q_{21} branches need not be considered because their contributions are very small, if they exist at all. The calculation for the absorption coefficient for a band belonging to Hund's case (a) would use line strengths of m/8 for the eight P and R branches and m/4 for the four Q branches. For the transitional nitric oxide γ series all the intricacies of the expressions for the line strengths must be taken into account.

If one substitutes values for the line strength, and $dm/d\nu$ into equation (11), the absorption coefficient is obtained for the 12 branches. A typical equation is given for the P_1 branch by

$$A_{P_1} = \frac{\left\{ m/8 + 1/16 \, \frac{(4m^2 - 2\lambda)}{(4m^2 - 4\lambda + \lambda^2)^{1/2}} \right\} \exp\left(-m^2 B_{eff}^{(1)} hc/kT\right)}{-(2B' + B_{eff}^{(0)}) + 2m\,(B' - B_{eff}^{(1)})} \tag{20}$$

A calculation for the absorption coefficient was carried out for a temperature of 473°K. The 12 equations of the form (20) and the 12 branch equations, were computed for values of m. The contributions from the branches are given in figure III and the summed intensity of the absorption coefficient of the band is given in figure IV.

The length of this calculation and the difficulties involved in representing the absorption coefficient as a function of $\Delta\nu$ is directly attributable to the complexity of the expressions for line strengths. The absorption coefficient envelope can be reproduced if the rotational constants, B and the temperature are known, but the analysis of experimental values using expressions of the form of equation (20) to obtain temperatures would be nearly impossible.

FIRST-ORDER APPROXIMATION

To obtain a single expression for the absorption coefficient in terms of $\Delta\nu$ band head, an approximate solution was carried out for equations of the form of equation (20) in the wing of the sub-band composed of branches P_2, R_2, Q_2, P_{12}, R_{12} and Q_{12}. In this treatment those parts of the line strength expressions which are not linearly dependent on m were expanded in a Taylor's series about the point $\lambda^{1/2}$. The series expansions was carried only to the first order to avoid introducing higher powers of m. In this form it was possible to represent the absorption coefficient as a function of $\Delta\nu$. Several points were calculated for T equal to 473°K and are indicated in figure IV.

THE SINGLET MODEL (ref. (1))

From the data it is apparent that the region of the band most noticeably affected by the temperature is the wings or the region for $\Delta\nu$ band head greater than 50. If one again examines the equations for the line strength, it is seen that for large values of m the P_1, Q_1, R_1, P_2, Q_2, and R_2 branches dominate and the P_{12}, Q_{12}, R_{12}, P_{21}, Q_{21}, and R_{21} branches vanish. It is also seen that values for the density of states, $dm/d(\Delta\nu)$ depend only on the m term. Therefore, in the region of large M, even for this transitional case, the absorption coefficient approaches the singlet-like representation. It is not readily apparent from the equations where agreement between the two models begins. The use of a singlet model for representing the wings of the nitric oxide γ_{00} band would simplify the reduction of experimental data.

For the singlet transition $^1\Sigma \rightarrow {}^1\Pi$ the terms are simply

$$F'(J) = B'J(J+1),$$
$$F''(J) = B''J(J+1). \tag{21}$$

The branch equations are

$$P \qquad \nu = \nu_0 - (B'+B'')J + (B'-B'')J^2, \tag{22a}$$

$$Q \qquad \nu = \nu_0 + (B'-B'')J + (B'-B'')J^2, \tag{22b}$$

$$R \qquad \nu = \nu_0 + 2B' + (3B'-B'') + (B'-B'')J^2. \tag{22c}$$

For this set of branch equations, only the P branch is head-forming. In the calculation of the band the intensities of the three branches are repeated at the doublet separation. The contribution from the extreme wings of the initial sub-band is taken into account.

The line strengths for the branches are given by the Hönl-London relations (ref. (1)). For the $^2\Sigma \rightarrow {}^2\Pi$ transition they are

$$S_P = (J''-2)(J''-1)/4J'', \tag{23a}$$

$$S_Q = (J''+2)(J''-1)(2J''+1)/4J''(J''+1) \tag{23b}$$

$$S_R = (J''+3)(J''+2)/4(J''+1) \tag{23c}$$

For the simple singlet model they are approximated by

$$S_P = S_R = m/4, \tag{24a}$$

$$S_Q = m/2. \tag{24b}$$

These values for the line strengths and values of $dm/d(\Delta\nu)$ obtained from the branches, equations (22) give the absorption coefficient. The equation for the P branch is

$$A_P = \frac{m/4 \exp.(-m^2 B'' hc/kT)}{-(B'+B'') + 2m(B'-B'')} \quad (25)$$

Equations for the R and Q branches are similar. To obtain a single equation for absorption coefficient the branch equations are solved for m in terms of $\Delta\nu$ band head and summed. The value of $\Delta\nu$ band head is found by differentiating the P branch equation and finding the value of the rotational quantum number at the turning point. This value, substituted into the P branch equation, yields the distance in wave numbers from the band origin to the band head. The coordinates of the band are shifted by that value and m is determined in terms of $\Delta\nu$ band head. The $\Delta\nu$ band head representation for the absorption coefficient becomes

$$A = \frac{1/4\left\{\frac{B'+B''}{2(B'-B'')} \pm \sqrt{\frac{\Delta\nu_{BH}}{B'-B''}}\right\} \exp.\left[-\left(\frac{B'+B''}{2(B'-B'')} \pm \sqrt{\frac{\Delta\nu_{BH}}{B'-B''}}\right)^2 B'' hc/kT\right]}{\sqrt{4(B'-B'')\Delta\nu_{BH}}}$$

$$+ \frac{1/4\left\{-\frac{(3B'-B'')}{2(B'-B'')} + \sqrt{\frac{\Delta\nu_{BH}}{B'-B''}}\right\} \exp.\left[-\left(-\frac{(3B'-B'')}{2(B'-B'')} + \sqrt{\frac{\Delta\nu_{BH}}{B'-B''}}\right)^2 B'' hc/kT\right]}{\sqrt{4(B'-B'')\Delta\nu_{BH}}} \quad (26)$$

$$+ \frac{1/2\left\{-1/2 + \sqrt{\frac{\Delta\nu_{BH}}{B'-B''} - \frac{B''}{(B'-B'')}}\right\} \exp.\left[-\left(-1/2 + \sqrt{\frac{\Delta\nu_{BH}}{B'-B''} - \frac{B''}{(B'-B'')}}\right)^2 B'' hc/kT\right]}{\sqrt{4(B'-B'')\Delta\nu_{BH} + B''}}$$

This form of the equation gives the absorption coefficient directly. The value of B' is the same used for the doublet calculation. The value for B" is the average value of B_{eff}^1 and B_{eff}^2.

The singlet model is used to calculate the absorption coefficient for temperatures of 300°K, 373°K, 473°K and 573°K. The plot of the absorption coefficient for the temperature 473°K is given in figure IV. Figure IV indicates close agreement between the three models for the nitric oxide γ_{00} band in the wing. The calculations for the intensity of absorption for the four temperatures were made using the absorption coefficients obtained from the singlet model which provides a simpler method for interpretation of experimental values.

Section 5

RESULTS

The curves for the intensity of absorption are obtained from equation (10). The singlet model is used to determine absorption coefficients. The curves which correspond to the four experimental temperatures are plotted in figures VII through X, together with the experimental data. There is an agreement between predicted and experimental values. This agreement begins at approximately $\Delta\nu$ band head equal to 40 cm^{-1} for the sub-band headed by the P_{12} branch. Agreement for the sub-band headed by the P_1 branch begins at $\Delta\nu$ band head approximately equal to 150 cm^{-1} (see figure (II)). A comparison of absorption coefficients for the doublet and singlet models indicated that for the sub-band headed by the P_{12} branch agreement should not begin until $\Delta\nu$ band head is equal to approximately 55 cm^{-1}. This apparent discrepancy can only be accounted for by experimental scatter and by the averaging effect of the spectroscopic resolution.

If one compares experimental results with the curves calculated from the singlet model one finds large discrepancies in the region of the band heads. These discrepancies are accounted for by the differences between the doublet representation and the singlet model and are entirely expected, with one exception. In the region between the P_{12} band head and the origin measured values of the intensity of absorption are greater than the values predicted by the doublet model. This discrepancy is accounted for by the differences between J and m. The difference would give a larger percentage error for small values of m. In other parts of the band, even in regions of small m, a number of branches are superimposed, apparently reducing the error.

Section 6

DISCUSSION

TEMPERATURE MEASUREMENTS

The experimental and computed values have been obtained for known temperatures. The question of interpretation of experimental data when there is an absence of temperature values still remains. It is conceivable that the ratio of the relative absorption coefficient for two values of $\Delta\nu$ can be calculated for a number of temperatures and a calibration curve plotted. This technique limits the taking of experimental data to two points and presents the possibility of large experimental

errors. A second approach would be to examine the available values, both experimental and theoretical, and determine if some property exists which lends readily to the determination of temperatures.

If one takes the natural logarithm of the absorption coefficient and plots these values against $\Delta\nu$, it is immediately seen that the plot is very nearly linear in the wings of the band. For very large values of $\Delta\nu$ equation (26) becomes (ref. (4))

$$A = \frac{\exp\left\{\left[-\Delta\nu B''/(B'-B'')\right]\left[hc/kT\right]\right\}}{2(B'-B'')} \tag{27}$$

Then it follows

$$d(\log A)/d(\Delta\nu) = -\left[B''/(B'-B'')\right]\left[hc/kT\right] \tag{28}$$

This modified form of equation (26) yielded errors of the order of 30 percent for temperature.

To determine the source of the errors and find a correction, $d(\log A)/d(\Delta\nu)$ was directly arrived at from equation (26) without first making the assumption of large values of $\Delta\nu$. The equation for $d(\log A)/d(\Delta\nu)$ is

$$\begin{aligned} d(\log A)/d(\Delta\nu) = {} & -\frac{B''}{B'-B''}\frac{hc}{kT} + \frac{\frac{B''}{B'-B''}\frac{hc}{kT}\left[-\frac{(B'+B'')}{(B'-B'')}A_P + \frac{(3B'-B'')}{(B'-B'')}A_R\right]}{A\sqrt{4(B'-B'')\Delta\nu}} \\ & + \frac{\frac{B''}{(B'-B'')}\frac{hc}{kT}A_Q}{A\sqrt{4(B'-B'')\Delta\nu - 4B'B''}} - \frac{\left[2(B'-B'')A_P + 2(B'-B'')A_R\right]}{A\,4(B'-B'')\Delta\nu} \\ & - \frac{2(B'-B'')A_Q}{A\left[4(B'-B'')\Delta\nu - 4B'B''\right]} + \frac{2A_P(B'-B'')}{\left[(B'+B'') + \sqrt{4(B'-B'')\Delta\nu}\right]\sqrt{4(B'-B'')\Delta\nu}} \\ & + \frac{2A_R(B'-B'')}{\left[-(3B'-B'') + \sqrt{4(B'-B'')\Delta\nu}\right]\sqrt{4(B'-B'')\Delta\nu}} + \frac{2A_Q(B'-B'')}{\left[-(B'-B'') + \sqrt{4(B'-B'')\Delta\nu - 4B'B''}\right]\sqrt{4(B'-B'')\Delta\nu - 4B'B''}} \end{aligned} \tag{29}$$

Simplifying assumptions are made to reduce equation (26) to a usable form. We first consider only the zeroth and first order terms, i.e., the linear term and terms which are inversely dependent on the square root of $\Delta\nu$. Secondly, we make the assumption that in the region under consideration the P branch contributes a negligible amount to the absorption coefficient and that the contributions of the R and Q branches are nearly equal. A simplified form of equation (29) is then

$$d(\log A)/d(\Delta\nu) \approx -\frac{B''}{B'-B''}\frac{hc}{kT}\left[1-\frac{(2B'-B'')}{\sqrt{4(B'-B'')\Delta\nu}}\right]. \qquad (30)$$

The values of temperature found from the experimental results using equation (30) are included in Table I. Agreement with values measured with the thermocouple was better than 6 percent.

DETERMINATION OF ROTATIONAL CONSTANTS

In addition to equation (30) there exists a second equation in terms of the rotational constants. This is the equation for the separation of the band head from the band origin. For the P_{12} head-forming branch the relation is,

$$\Delta\nu = 3/4B' - \frac{(2B'+B_{eff}^{(2)})^2}{4(B'-B_{eff}^{(2)})}, \qquad (31)$$

with the assumption that $B_{eff}^{(2)} \approx B''$. The value of $\Delta\nu$ measured from the data is - 26 cm^{-1}. If it is assumed now that temperature is known, one has two equations in two unknowns. Equations (30) and (31) are solved most readily by an iterative method. Initial values of the rotational constants are derived using equation (31) and the linear term from equation (30). The values thus obtained are substituted in the nonlinear corrective term in equation (30) and the rotational constants recalculated.

The values obtained for the first approximation are $B' = 2.41\ cm^{-1}$, an error of 21 percent and $B'' = 1.99\ cm^{-1}$, an error of 16 percent. The values of the rotational constants found after the corrections are $B' = 1.73\ cm^{-1}$, an error of 13 percent and $B'' = 1.58\ cm^{-1}$, an error of 6 percent. The value of - 26 cm^{-1}, used in equation (28), is known to be in error. The exact value is - 28. 7 cm^{-1}. However, the P_2, Q_{12} band head is superimposed on the band origin making its exact location difficult to determine. If an accurate determination of $\Delta\nu$ in equation (31) was possible the values of the rotational constants would have been $B' = 1.88\ cm^{-1}$, an error

of 5 percent and B" = 1.61, an error of 4 percent. These errors are of the same order as errors in determination of temperature. Had the nitric oxide δ_{00} band been a singlet transition, the band origin would not have been obscured by the second band head and the determination of rotational constants would have been more accurate.

CONCLUSION

If the experimental problem is only the determination of temperature, there is available a large number of diatomic molecules for which molecular rotational constants and electronic terms are well known. The choice of a molecular species should be determined by three factors. The first, of course, is the existence of the molecule in the experimental environment. The second factor is to choose a molecule which has a band in a relatively uncluttered region of the spectrum and whose constants provide a band of size, shape, and intensity which facilitates the measurements. The third factor, and least important, is that the molecule should, if possible, be a singlet electronic transition or one which belongs to Hund's dase (b).

The nitric oxide molecule is not a good choice with respect to the third consideration and necessitates a more detailed treatment than might have been required for a simpler molecule. However, if as in this investigation the choice is limited, a simple model of the more complicated band may suffice.

The determination of molecular constants is, in a sense, a by-product of the investigation. For the most part, equation (31) is not as easily determined as is equation (30). Spectrographic resolution and band-head overlap tend to obscure the band origin. The determination of these constants, however, even to accuracies of the order of 13 percent would be useful for measurements made for unstable molecules whose existence is of so short a duration that the use of a high resolution instrument would not be feasible. The determination of a molecular constant to 13 percent accuracy leads to the determination of the internuclear distance r to the order of 7 percent accuracy. Such measurements are desirable when there exists no other methods for obtaining the experimental information.

REFERENCES

(1) Herzberg, G., Spectra of Diatomic Molecules, Van Nostrand, Princeton, New Jersey, 1950

(2) Jevons, W., Band Spectra of Diatomic Molecules, Physical Society, London, 1932

(3) Schiff, L. I., Quantum Mechanics, McGraw-Hill, New York, 1949

(4) Marshall, T., Intensity Distribution in Unresolved Electronic Bands of Diatomic and Symmetric Top Molecules, Doctoral Dissertation, 1962

(5) Dickerman, P. J., Optical Spectrometric Measurements of High Temperatures
Phillips, J. G., Measurement of Gaseous Temperatures Below 8000°K, University of Chicago Press, Chicago, 1961

(6) Guillery, M., Z. Physik, 42, 121, 1927

(7) Schmid, R., Z. Physik, 49, 428, 1928

(8) Mulliken, R. S., Phys. Rev., 32, 388, 1928

(9) Earls, L. T., Phys. Rev., 48, 423, 1935

(10) Pearse, R. W. B., and Gaydon, A. G., The Identification of Molecular Spectra, Wiley, New York, 1950

(11) Penner, S. S., Quantitative Molecular Spectroscopy and Gas Emissivities, Addison-Wesley, Reading, Mass., 1959

(12) White, H. E., Introduction to Atomic Spectra, McGraw-Hill, New York, 1934

(13) Pomerantz, J., The Influence of the Absorption of Radiation in Shock Tube Phenomena, NavOrd Rept. 6136, 1958

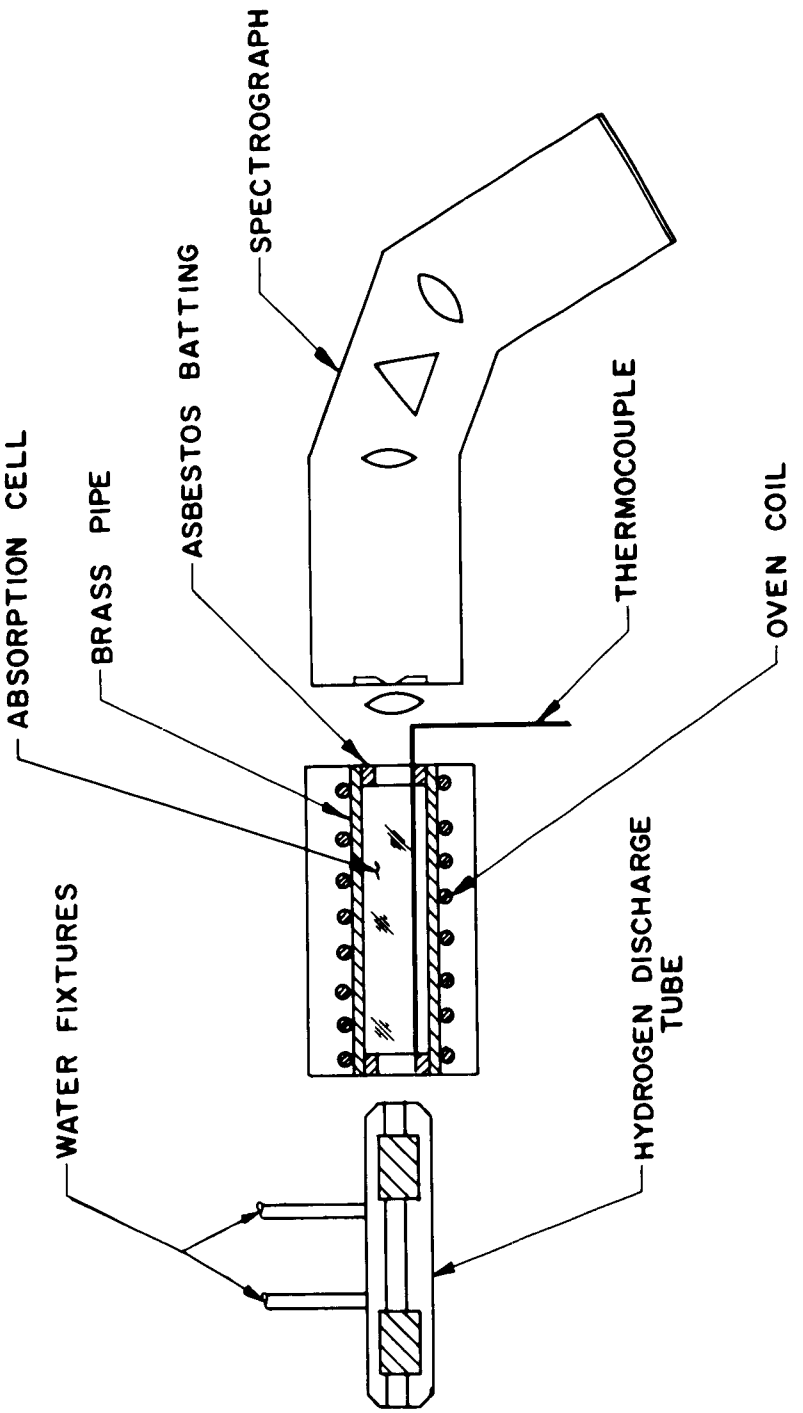

FIGURE I EXPERIMENTAL APPARATUS

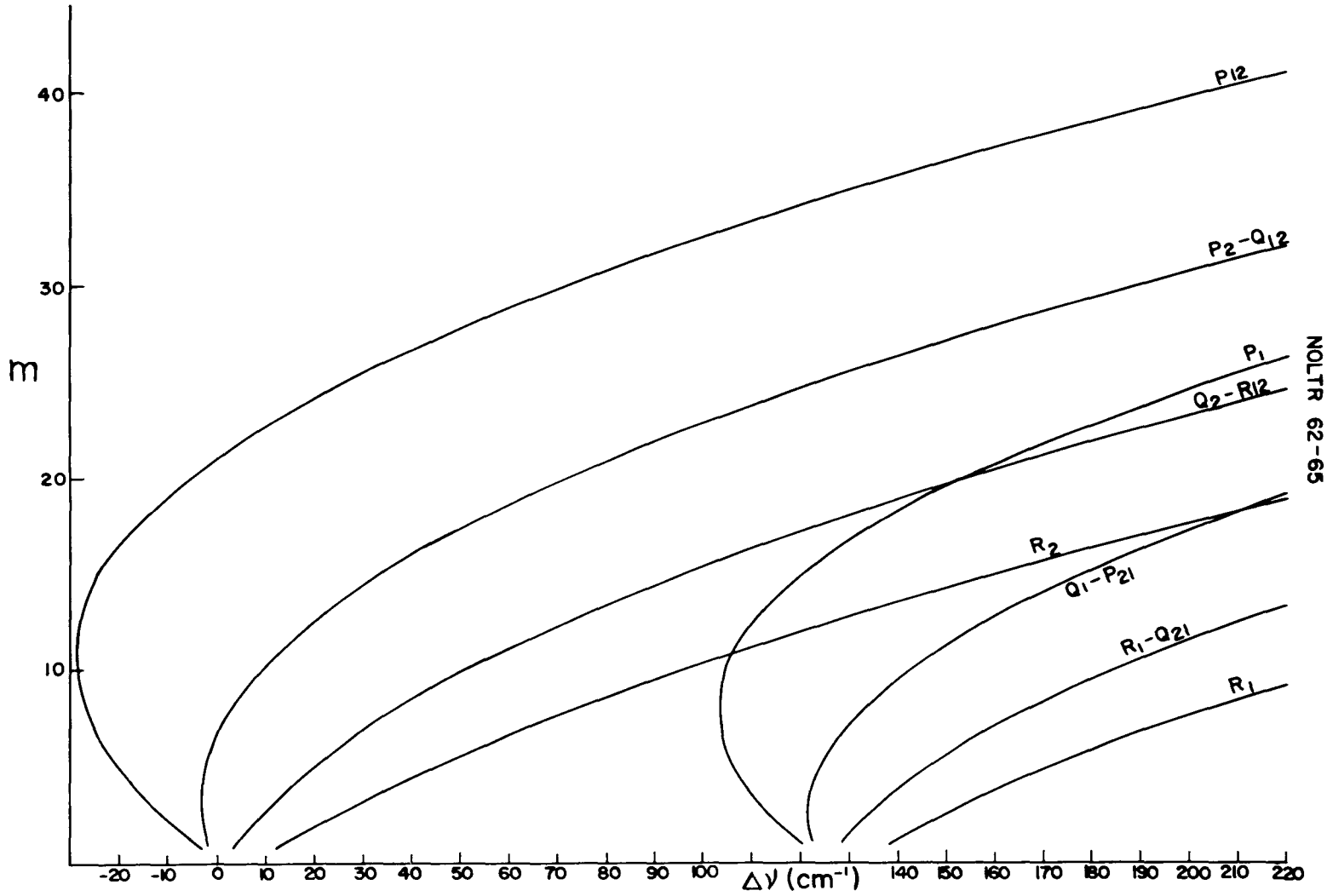

FIGURE II FORTRAT DIAGRAM FOR THE NITRIC OXIDE γoo BAND

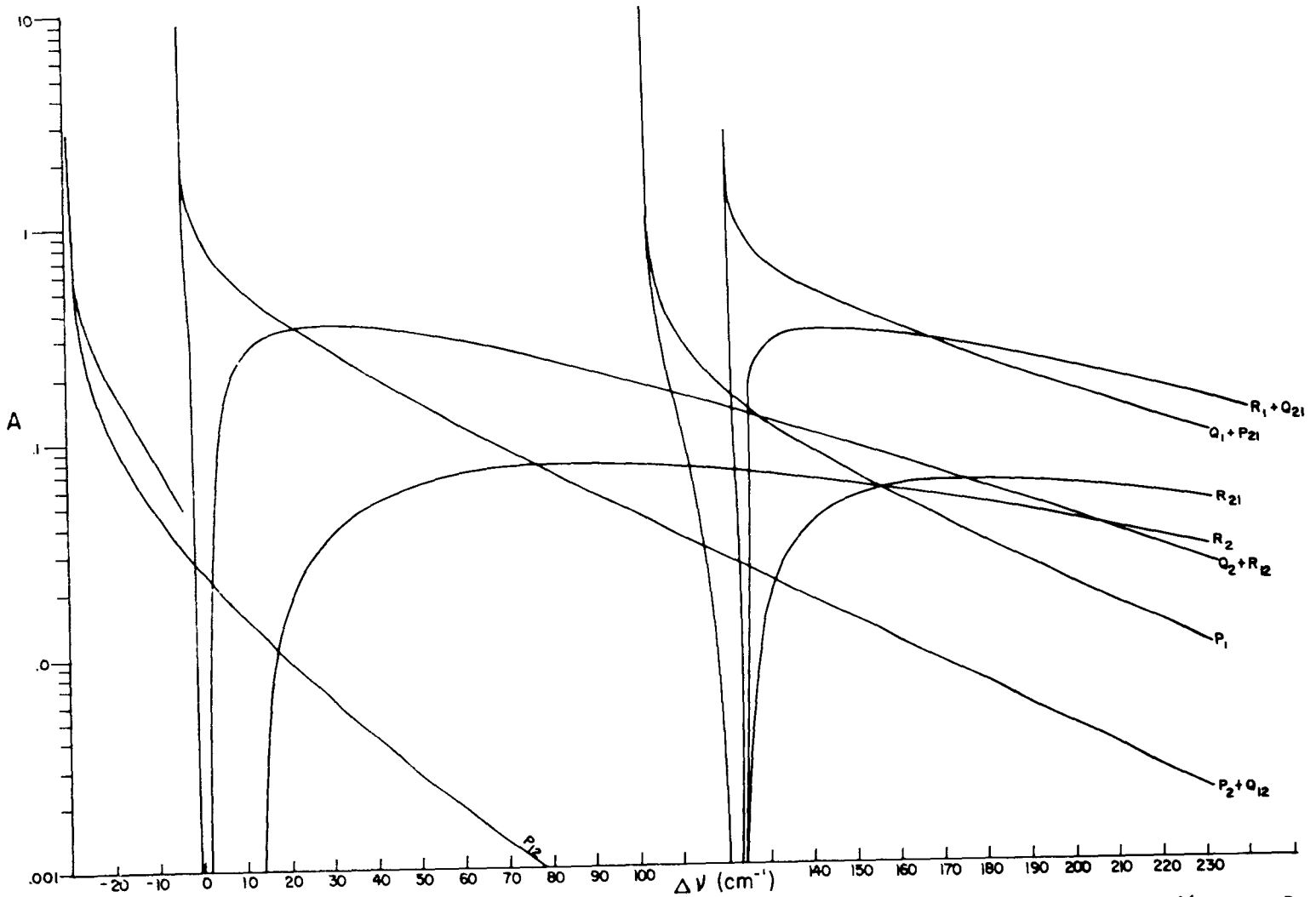

FIGURE III ABSORPTION COEFFICIENT FOR THE BRANCHES OF THE NITRIC OXIDE γ_{oo} BAND

NOLTR 62-65

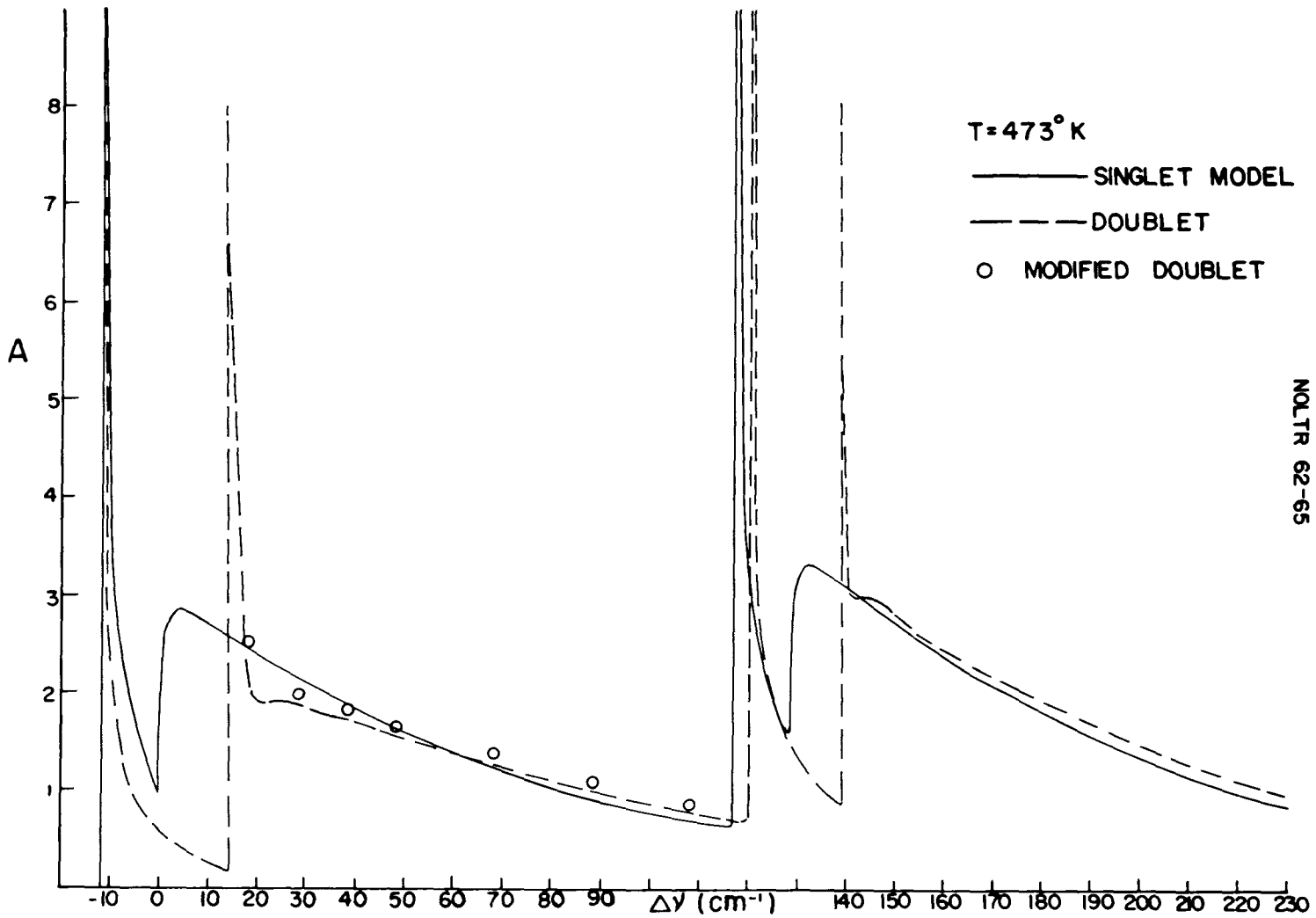

FIGURE IV ABSORPTION COEFFICIENT FOR THE THREE MODELS OF THE NITRIC OXIDE γ_{00} BAND

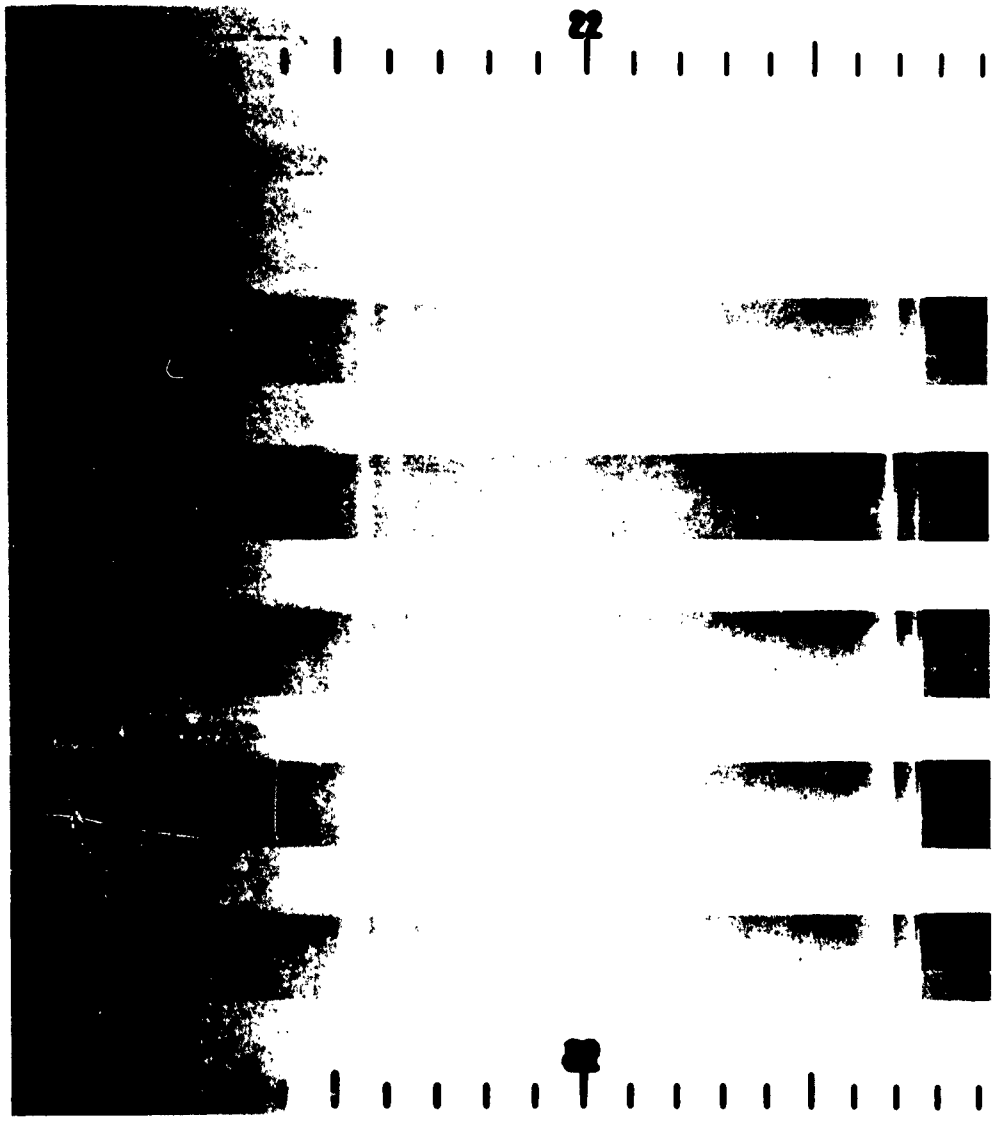

FIG. 5 SPECTROGRAPHIC PLATE FOR SIX RUNS

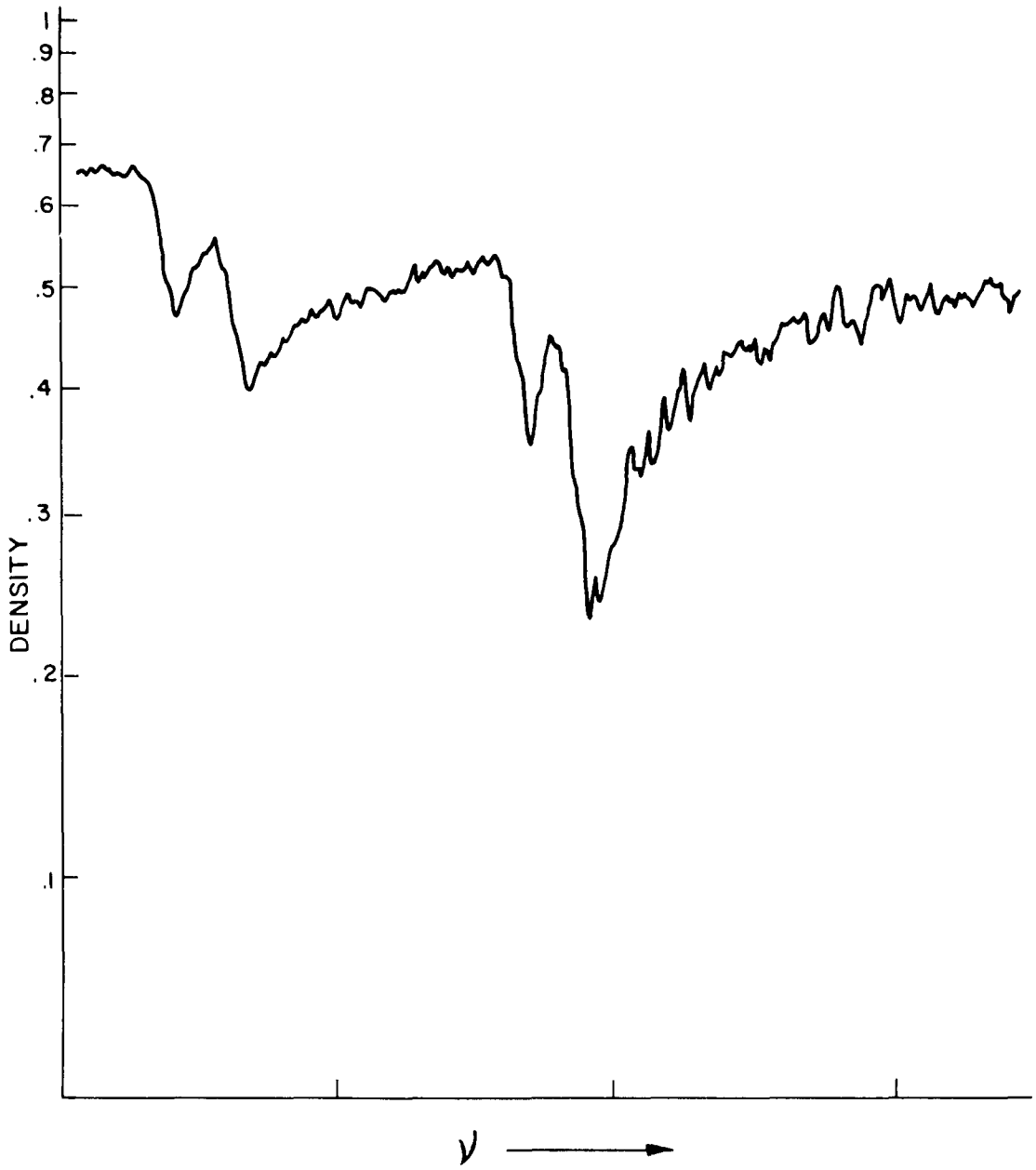

FIGURE VI TYPICAL DENSITOMETER TRACE

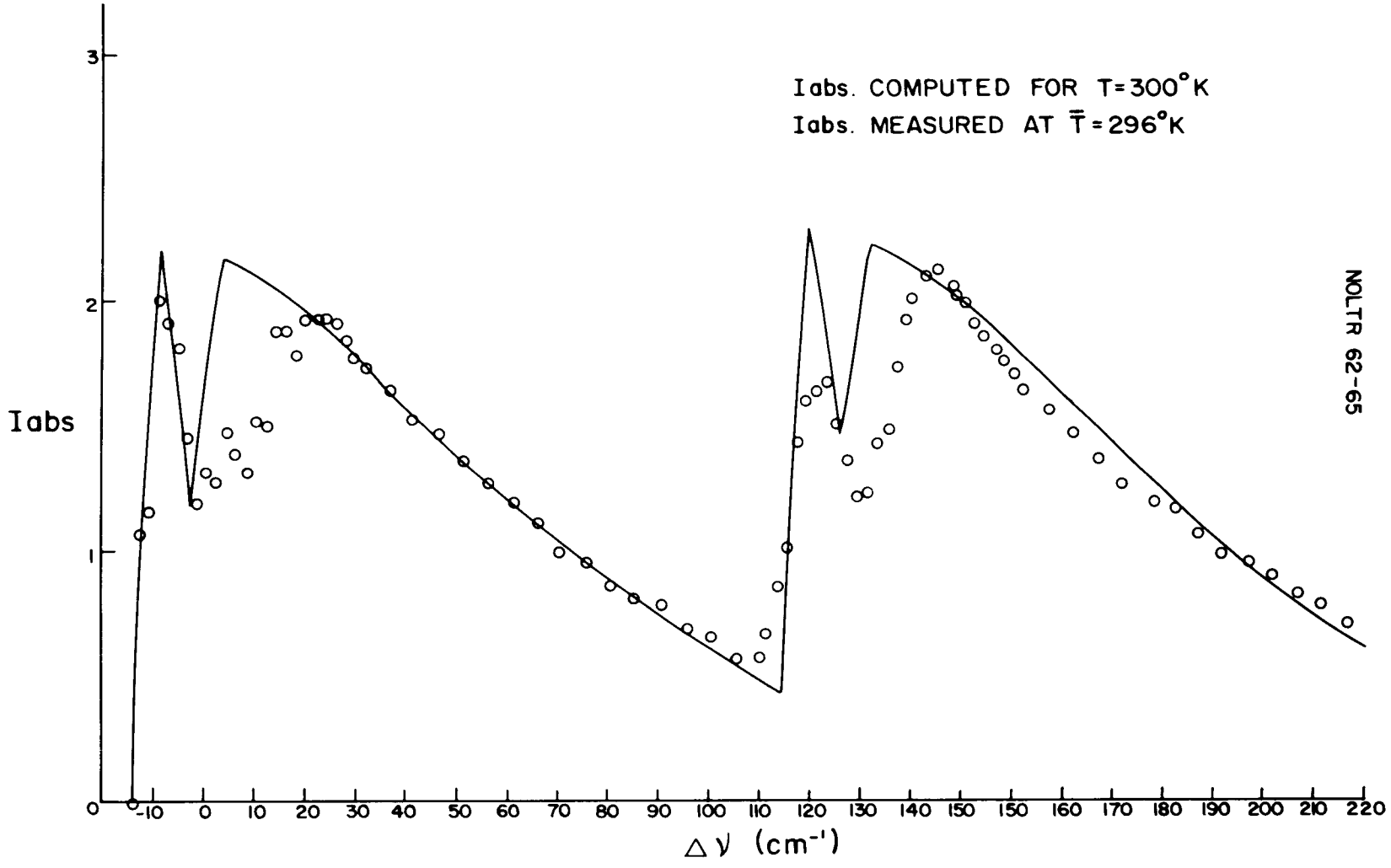

FIGURE VII INTENSITY OF ABSORPTION RUN NUMBER 2

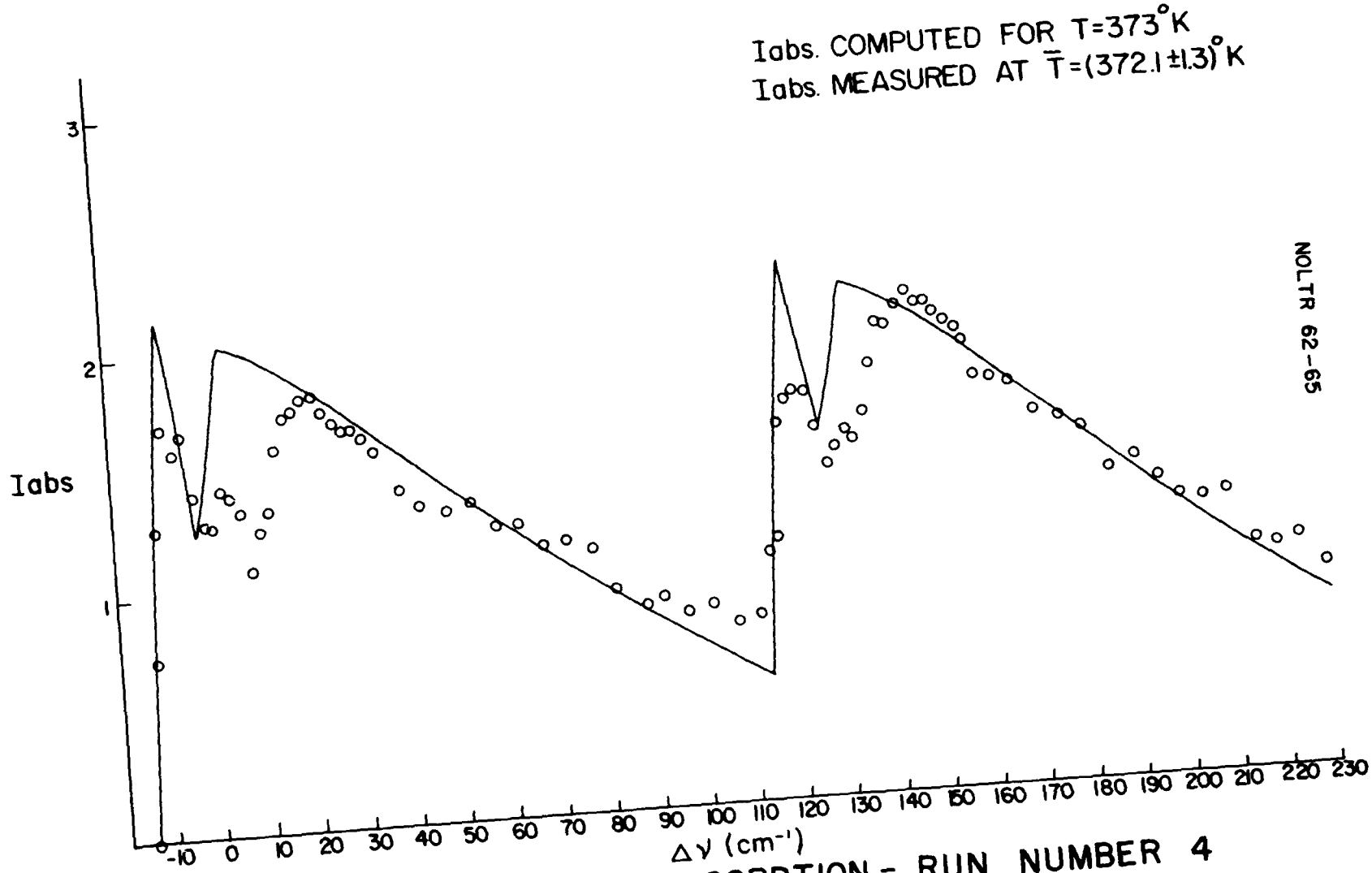

FIGURE VIII INTENSITY OF ABSORPTION - RUN NUMBER 4

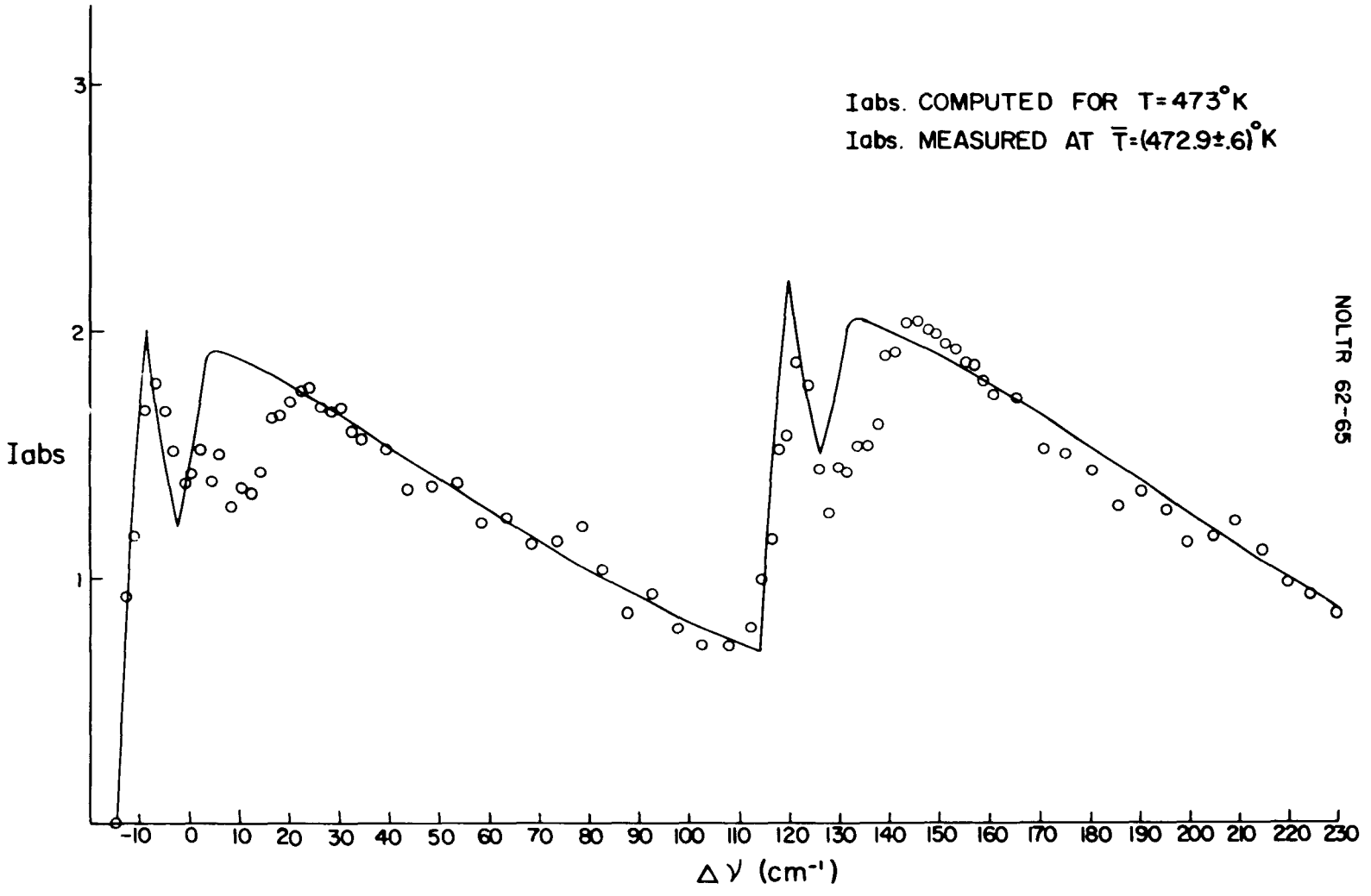

FIGURE IX INTENSITY OF ABSORPTION – RUN NUMBER 5

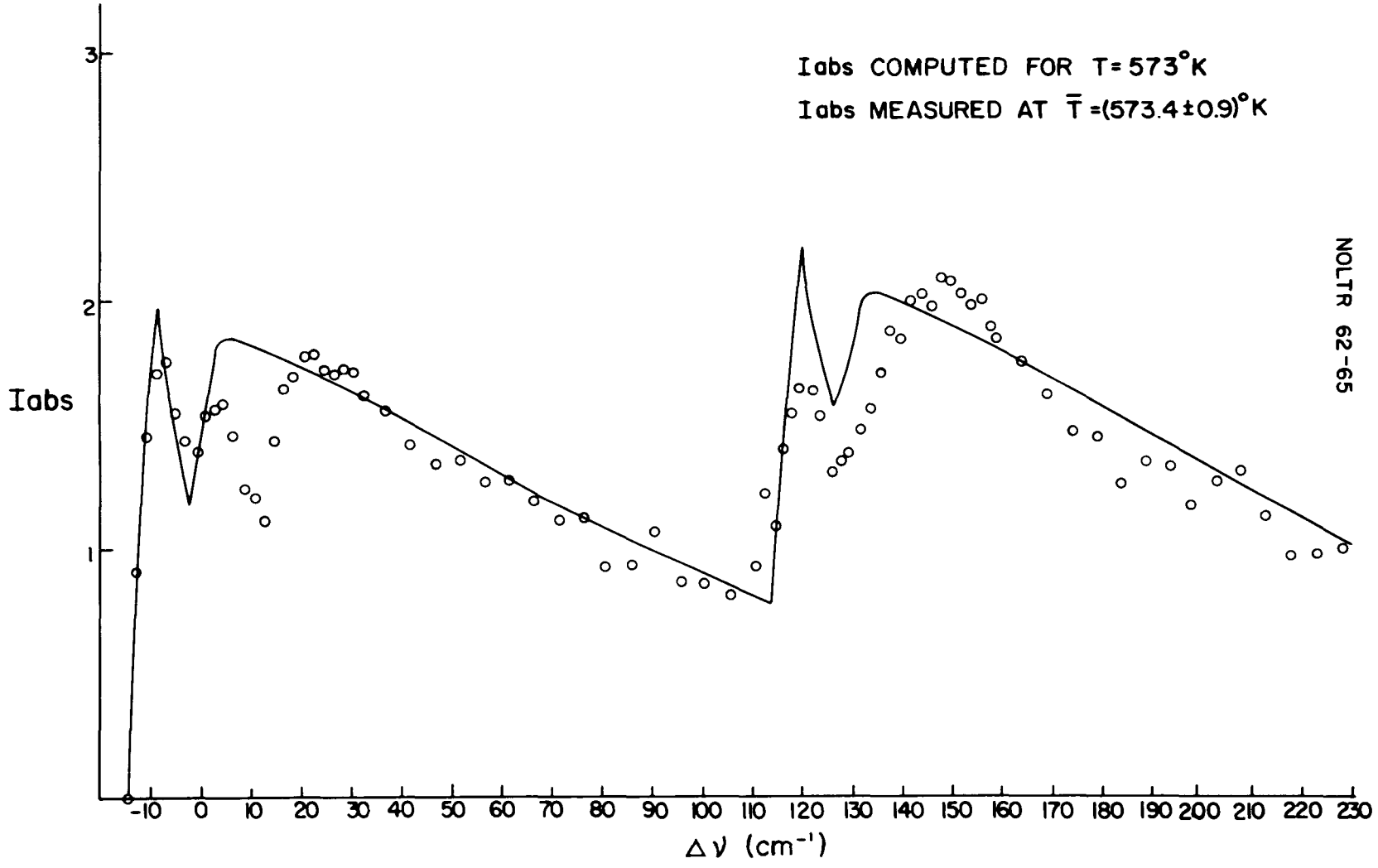

FIGURE X INTENSITY OF ABSORPTION – RUN NUMBER 6

TABLE I: EXPERIMENTAL TEMPERATURES AND OTHER PERTINENT DATA

Run No.	Slit Width	Exposure Time	Temperature Thermocouple	$\frac{d(\log A)}{d(\Delta\nu)}$ ($\Delta\nu = 900\,cm^{-1}$)	Temperature Spectrographic	% Deviation
1	10 Microns	32 Minutes	296±0°K			
2	20 Microns	16 Minutes	296±0°K	-.0229	313°K	5.7%
3	40 Microns	8 Minutes	296±0°K			
4	20 Microns	16 Minutes	372.1±1.3°K	-.0182	393°K	5.6%
5	20 Microns	16 Minutes	472.9±0.6°K	-.0146	492°K	4.0%
6	20 Microns	16 Minutes	573.4±0.1°K	-.0123	582°K	1.5%

TABLE II: DENSITOMETER DATA: RUN NUMBER 1

$\Delta\nu$ (cm^{-1})	$I_{abs.}$	$\Delta\nu$ (cm^{-1})	$I_{abs.}$	$\Delta\nu$ (cm^{-1})	$I_{abs.}$	$\Delta\nu$ (cm^{-1})	$I_{abs.}$
-14.60	0	35.73	3.5	128.35	4.1	218.05	2.0
-14.00	3.5	40.60	3.2	130.30	5.2	222.93	1.8
-12.05	4.1	45.48	3.0	132.25	5.7	227.80	1.7
-10.10	4.1	50.35	3.0	134.20	5.9	232.68	1.5
-8.15	3.9	55.23	2.6	136.15	6.0		
-6.20	3.4	60.10	2.4	138.10	6.0		
-4.25	2.9	64.98	2.2	140.05	5.5		
-2.30	2.5	69.85	2.1	142.00	5.4		
-0.35	2.3	74.73	2.0	143.95	5.3		
1.60	2.2	79.60	2.0	145.90	5.2		
3.55	2.2	84.48	1.8	147.85	5.0		
5.50	2.0	89.35	2.1	149.80	4.9		
7.45	2.8	94.23	2.0	154.68	4.4		
9.40	4.5	99.10	1.9	159.55	4.2		
11.35	5.0	103.98	1.7	164.43	3.9		
13.30	4.9	108.85	1.7	169.30	3.7		
15.25	4.8	110.80	2.1	174.18	3.5		
17.20	4.5	112.75	4.0	179.05	3.4		
19.15	4.5	114.70	4.3	183.93	3.1		
21.10	4.3	116.65	4.4	188.80	3.1		
23.05	4.2	118.60	3.9	193.68	2.7		
25.00	4.1	120.55	3.8	198.55	2.5		
26.95	4.0	122.50	3.2	203.43	2.4		
28.90	3.8	124.45	2.9	208.30	2.3		
30.85	3.8	126.40	3.2	213.18	2.1		

TABLE III: DENSITOMETER DATA: RUN NUMBER 2

$\Delta\nu$ (cm^{-1})	$I_{abs.}$	$\Delta\nu$ (cm^{-1})	$I_{abs.}$	$\Delta\nu$ (cm^{-1})	$I_{abs.}$	$\Delta\nu$ (cm^{-1})	$I_{abs.}$
-14.60	0	31.83	13.6	126.40	11.0	198.55	9.4
-14.00	6.0	36.70	12.7	128.35	9.7	203.43	8.9
-12.05	10.1	41.58	12.0	130.30	11.2	208.30	8.5
-10.10	13.0	46.45	11.1	132.25	12.0	213.18	8.0
-8.15	13.9	51.33	10.7	134.20	14.3	218.05	7.5
-6.20	14.4	56.20	10.0	136.15	16.7	222.93	7.0
-4.25	13.0	61.08	9.3	138.10	17.3	227.80	6.5
-2.30	11.0	65.95	8.2	140.05	18.6	232.68	6.1
-0.35	10.1	70.83	7.7	142.00	19.1		
1.60	8.6	74.73	6.9	143.95	18.7		
3.55	8.8	79.60	6.4	145.90	18.5		
5.50	7.8	84.48	6.6	147.85	18.3		
7.45	7.8	89.25	5.9	149.80	17.8		
9.40	9.6	94.23	5.3	151.75	17.4		
11.35	10.0	99.10	4.9	153.70	17.0		
13.30	13.8	103.98	4.2	155.65	16.5		
15.25	14.9	108.85	5.0	157.60	16.0		
17.20	14.9	110.80	6.5	159.55	15.4		
19.15	16.0	112.75	7.8	164.43	14.6		
21.10	16.0	114.70	11.5	169.30	14.3		
23.05	16.1	116.65	13.4	174.18	13.3		
25.00	15.6	118.60	14.3	179.05	12.4		
26.95	15.3	120.55	14.9	183.93	11.3		
28.90	14.7	122.50	13.9	188.80	10.9		
30.85	14.5	124.45	13.3	193.68	10.1		

TABLE IV: DENSITOMETER DATA: RUN NUMBER 3

$\Delta\nu(cm^{-1})$	$I_{abs.}$	$\Delta\nu(cm^{-1})$	$I_{abs.}$	$\Delta\nu(cm^{-1})$	$I_{abs.}$	$\Delta\nu(cm^{-1})$	$I_{abs.}$
-14.60	0	35.73	17.2	128.35	16.4	218.05	9.2
-14.00	6.0	40.60	16.8	130.30	19.1	222.93	8.5
-12.05	8.7	45.48	15.5	132.25	22.2	227.80	8.1
-10.10	13.8	50.35	15.1	134.20	25.7	232.68	7.2
-8.15	17.1	55.23	14.2	136.15	26.4		
-6.20	17.2	60.10	13.4	138.10	26.9		
-4.25	17.8	64.98	12.4	140.05	26.9		
-2.30	15.4	69.85	11.4	142.00	26.5		
-0.35	12.8	74.73	10.6	143.95	26.1		
1.60	12.5	79.60	9.9	145.90	25.1		
3.55	10.2	84.48	9.1	147.85	23.9		
5.50	9.6	89.35	8.7	149.80	23.1		
7.45	10.0	94.23	8.0	154.68	22.6		
9.40	13.6	99.10	7.2	159.55	21.4		
11.35	16.5	103.98	6.7	164.43	19.9		
13.30	19.3	108.85	6.0	169.30	18.8		
15.25	20.5	110.80	9.9	174.18	17.6		
17.20	22.2	112.75	14.1	179.05	15.5		
19.15	22.5	114.70	17.6	183.93	14.8		
21.10	21.6	116.65	19.5	188.80	13.9		
23.05	21.1	118.60	20.8	193.68	13.3		
25.00	20.2	120.55	20.9	198.55	12.3		
26.95	19.2	122.50	17.8	203.43	11.6		
28.90	19.0	124.45	17.2	208.30	10.7		
30.85	18.4	126.40	15.8	213.18	10.0		

TABLE V: DENSITOMETER DATA: RUN NUMBER 4

$\Delta\nu$(cm^{-1})	$I_{abs.}$	$\Delta\nu$(cm^{-1})	$I_{abs.}$	$\Delta\nu$(cm^{-1})	$I_{abs.}$	$\Delta\nu$(cm^{-1})	$I_{abs.}$
-14.6	0	34.15	15.8	129.70	13.1	204.78	11.7
-12.65	5.1	39.03	14.1	131.65	13.0	209.65	11.9
-10.70	9.4	43.90	13.4	133.60	13.1	214.53	9.7
-8.75	13.7	48.78	13.2	135.55	14.4	219.40	9.6
-6.80	13.9	53.65	13.5	137.50	16.4	224.28	9.9
-4.85	16.3	58.53	12.3	139.45	18.4	229.15	8.7
-2.90	15.3	64.40	12.5	141.40	18.6		
-0.95	14.5	68.28	11.4	143.35	19.7		
1.00	12.3	73.15	11.7	145.30	20.4		
2.95	11.8	78.03	11.3	147.25	19.9		
4.90	10.2	82.90	9.5	149.20	20.0		
6.85	9.1	87.78	8.8	151.15	19.6		
8.80	8.0	92.65	9.1	153.10	19.2		
10.75	9.7	97.53	8.5	155.05	18.9		
12.70	11.2	102.40	8.7	157.00	18.4		
14.65	14.2	107.28	7.9	158.95	16.9		
16.60	16.7	112.15	6.8	160.90	16.7		
18.55	17.6	114.10	8.5	165.78	16.6		
20.50	18.1	116.05	9.3	170.65	15.4		
22.45	18.3	118.00	13.9	175.53	15.2		
24.40	17.6	119.95	15.1	180.40	14.8		
26.35	17.1	121.90	16.4	185.28	13.0		
28.30	16.7	123.85	17.1	190.15	13.4		
30.25	16.8	125.80	16.0	195.03	12.6		
32.20	16.4	127.75	15.2	199.90	11.7		

TABLE VI: DENSITOMETER DATA: RUN NUMBER 5

$\Delta\nu$ (cm^{-1})	$I_{abs.}$	$\Delta\nu$ (cm^{-1})	$I_{abs.}$	$\Delta\nu$ (cm^{-1})	$I_{abs.}$	$\Delta\nu$ (cm^{-1})	$I_{abs.}$
-14.60	0	34.15	14.6	129.70	12.0	204.78	10.8
-12.65	3.3	39.025	14.2	131.65	11.2	209.65	11.4
-10.70	7.8	43.90	12.7	133.60	12.4	214.53	10.4
-8.75	12.3	48.78	12.8	135.55	12.7	219.40	9.2
-6.80	14.6	53.65	13.0	137.50	13.7	224.28	8.8
-4.85	15.1	58.53	11.4	139.45	16.3	229.15	8.2
-2.90	15.6	63.40	11.7	141.40	16.7		
-0.95	14.4	68.28	10.7	143.35	18.0		
1.00	12.3	73.15	10.8	145.30	18.3		
2.95	11.5	78.03	11.4	147.25	18.1		
4.90	9.5	82.90	9.8	149.20	18.0		
6.85	9.4	87.78	8.1	151.15	17.7		
8.80	8.6	92.65	9.0	153.10	17.4		
10.75	9.6	97.53	7.5	155.05	17.0		
12.70	10.4	102.40	6.9	157.00	16.9		
14.65	11.9	107.28	6.3	158.95	16.3		
16.60	14.8	112.15	6.4	160.90	15.8		
18.55	15.4	114.10	7.6	165.78	15.8		
20.50	15.9	116.05	9.0	170.65	13.9		
22.45	16.3	118.00	12.3	175.53	13.7		
24.40	16.5	119.95	13.4	180.40	13.1		
26.35	15.7	121.90	16.6	185.28	11.8		
28.30	15.6	123.85	16.5	190.15	12.5		
30.25	15.8	125.80	13.8	195.03	11.8		
32.20	14.9	127.75	12.8	199.90	10.6		

TABLE VII: DENSITOMETER DATA: RUN NUMBER 6

$\Delta\nu$ (cm^{-1})	$I_{abs.}$	$\Delta\nu$ (cm^{-1})	$I_{abs.}$	$\Delta\nu$ (cm^{-1})	$I_{abs.}$	$\Delta\nu$ (cm^{-1})	$I_{abs.}$
-14.60	0	34.15	14.5	129.70	10.9	204.78	11.4
-12.65	2.5	39.03	13.9	131.65	10.6	209.65	11.8
-10.70	5.8	43.90	12.7	133.60	11.6	214.53	10.1
-8.75	10.3	48.78	12.1	135.55	12.4	219.40	8.7
-6.80	13.4	53.65	12.2	137.50	13.9	224.28	8.7
-4.85	15.2	58.53	11.5	139.45	15.5	229.15	8.9
-2.90	15.5	63.40	11.5	141.40	15.6		
-0.95	14.3	68.28	10.8	143.35	17.1		
1.00	12.5	73.15	10.1	145.30	17.5		
2.95	11.2	78.03	10.6	147.25	17.2		
4.90	10.2	82.90	8.5	149.20	18.3		
6.85	9.5	87.78	8.5	151.15	18.1		
8.80	9.4	92.65	9.8	153.10	17.8		
10.75	8.5	97.53	8.0	155.05	17.4		
12.70	8.9	102.40	7.8	157.00	17.5		
14.65	9.3	107.28	6.9	158.95	16.6		
16.60	12.3	112.15§	7.1	160.90	16.3		
18.55	14.6	114.10	7.8	165.78	15.4		
20.50	15.1	116.05	8.2	170.65	14.3		
22.45	15.8	118.00	11.0	175.53	12.9		
24.40	15.9	119.95	12.7	180.40	12.7		
26.35	15.4	121.90	14.0	185.28	11.2		
28.30	15.2	123.85	14.7	190.15	12.0		
30.25	15.5	125.80	14.2	195.03	11.9		
32.20	15.3	127.75	12.7	199.90	10.5		

DISTRIBUTION

	Copies
Chief, Bureau of Naval Weapons Department of the Navy Washington 25, D. C.	
Attn: RMMO	1
Attn: RMGA	1
Attn: RRMA	1
Director, Special Projects Department of the Navy Washington 25, D. C.	
Attn: SP-20	4
Attn: SP-27	2
Attn: SP-272	1
Office of Naval Research Room 2709 - T-3 Washington 25, D. C.	
Attn: Head, Mechanics Br.	1
Commanding Officer Office of Naval Research Branch Office, Box 39, Navy 100 Fleet Post Office, New York, N. Y.	5
Director, DTMB Aerodynamics Laboratory Washington 7, D. C.	
Attn: Library	1
Naval Weapons Laboratory Dahlgren, Va.	
Attn: Library	1
Commander U. S. Naval Ordnance Test Station China Lake, Calif.	
Attn: Technical Library	1
Director Naval Research Laboratory Washington 25, D. C.	
Attn: Code 2027	1
Attn: Mr. Edward Chapin, Code 6310	1

	Copies
NASA Langley Research Center Langley Field, Va.	
Attn: Librarian	1
Attn: C. H. McLellan	1
Attn: J. J. Stack	1
Attn: Adolf Busemann	1
Attn: Rodger W. Peters (Structures Res. Div.)	1
Attn: Russell Hopko, PARD	1
NASA Ames Research Center Moffett Field, Calif.	
Attn: Librarian	1
NASA Lewis Research Center 21000 Brookpark Rd. Cleveland, Ohio	
Attn: Chief, Propulsion Aerodynamics Div.	1
Attn: Mr. George Mandel, Chief, Library	2
Office of the Assistant Secretary of Defense (R&D) Room 3E1041, The Pentagon Washington 25, D. C.	
Attn: Library (Technical)	1
Research and Development Board Room 3D1041, The Pentagon Washington 25, D. C.	
Attn: Library	2
ASTIA Arlington Hall Station Arlington 12, Va.	
Attn: TIPDR	10
Commander, Pacific Missile Range Point Mugu, Calif.	
Attn: Technical Library	1
Commanding General Aberdeen Proving Ground, Md.	
Attn: Technical Info. Br.	1
Attn: Ballistics Research Laboratories	1

	Copies
Director of Intelligence Headquarters, USAF Washington 25, D. C. Attn: AFOIN-3B	1
Commander Aeronautical Systems Division Wright-Patterson Air Force Base, Ohio	
Attn: WCOSI-3	2
Attn: WCLSW-5	1
Attn: WCRRD	3
Attn: Melvin L. Buck (ASRMDF-2)	1
Commander, AFBMD Air Res. & Develop. Command P. O. Box 262 Inglewood, Calif. Attn: WDTLAR	1
Chief, DASA The Pentagon Washington, D. C. Attn: Document Library	1
Headquarters Arnold Engineering Development Center (ARDC) U. S. Air Force Arnold Air Force Station, Tennessee	
Attn: Technical Library	1
Attn: AEOR	1
Commanding Officer, DOFL Washington 25, D. C. Attn: Library Rm. 211, Bldg. 92	1
NASA George C. Marshall Space Flight Center Huntsville, Alabama	
Attn: M-S&M-PT (Mr. H. A. Connell)	5
Attn: Dr. W. R. Lucas (M-SFM-M)	1
Attn: Dr. Ernst Geissler	1
Office, Chief of Ordnance Department of the Army Washington 25, D. C. Attn: ORDTU	1

	Copies
Institute for Defense Analyses Advanced Research Projects Agency Washington 25, D. C. Attn: W. G. May General Sciences Branch	1
Kaman Aircraft Corporation Nuclear Division Colorado Springs, Colorado Attn: Dr. A. P. Bridges	1
U. S. Atomic Energy Commission P. O. Box 62 Oak Ridge, Tennessee Attn: TRI:NLP:ATD:10-7	1
Sandia Corporation Livermore Laboratory P. O. Box 969 Livermore, Calif.	1
United Aircraft Corporation Research Laboratories East Hartford 8, Conn. Attn: Mr. H. J. Charette Attn: Mr. H. Taylor	1 1
Sandia Corporation Sandia Base Albuquerque, N. Mexico Attn: Mr. Alan Pope	1
Defense Metals Information Center Battelle Memorial Institute 505 King Avenue Columbus 1, Ohio	1
Commanding General Army Rocket and Guided Missile Agency Redstone Arsenal, Alabama Attn: John Morrow	1
National Bureau of Standards Washington 25, D. C. Attn: Dr. Galen B. Schubauer	1

	Copies
BSD(BSRP) A. F. Unit Post Office Los Angeles 45, Calif.	2
APL/JHU 8621 Georgia Ave. Silver Spring, Md.	
Attn: Tech. Reports Group	2
Attn: Dr. D. Fox	1
Attn: Dr. Freeman Hill	1
Attn: Dr. L. L. Cronvich	1
Attn: Librarian	1
AVCO Manufacturing Corp. Research & Advanced Development Div. 201 Lowell Street Wilmington, Mass.	
Attn: Dr. B. D. Henschel, Aerodynamics Section	1
General Electric Co. Space Vehicle & Missiles Dept. 21 South 12th St. Philadelphia, Penn.	
Attn: Dr. J. Stewart	1
Attn: Dr. Otto Klima	1
Attn: Mr. E. J. Nolan	1
Attn: Mr. L. McCreight	1
General Electric, Research Lab. 3198 Chestnut St. Philadelphia, Penn.	
Attn: Dr. Leo Steg	1
National Aeronautics and Space Admin. 1520 H Street, N. W. Washington, D. C.	5
NASA High Speed Flight Station Edwards Field, Calif.	
Attn: W. C. Williams	1
Aerospace Corporation El Segundo, Calif.	
Attn: Dr. Bitondo	1

	Copies
Lockheed Aircraft Corp. Missiles and Space Div. P. O. Box 504 Sunnyvale, Calif. Attn: Dr. L. H. Wilson	1
Lockheed Aircraft Corp. Research Lab. Palo Alto, California Attn: W. Griffith	1
Atomic Energy Commission Engineering Development Branch Division of Reactor Development Headquarters, US AEC Washington 25, D. C.	
Attn: Mr. J. M. Simmons	1
Attn: Mr. M. J. Whitman	1
Attn: Mr. J. Conners	1
University of California Lawrence Radiation Laboratory P. O. Box 808 Livermore, Calif.	
Attn: Mr. W. M. Wells, Propulsion Div.	1
Attn: Mr. Carl Kline	1
Oak Ridge National Laboratory P. O. Box E Oak Ridge, Tenn.	
Attn: Mr. W. D. Manly	1
General Applied Sciences Laboratories, Inc. Merrick and Stewart Avenues East Meadow, New York	
Attn: Mr. Robert Byrne	1
Jet Propulsion Laboratory 4800 Oak Grove Drive Pasadena 3, Calif.	
Attn: I. R. Kowlan, Chief, Reports Group	1
Attn: Dr. L. Jaffee	2
Los Alamos Scientific Laboratory P. O. Box 1663 Los Alamos, New Mexico	
Attn: Dr. Donald F. MacMillan N-1 Group Leader	1

	Copies
Cornell Aeronautical Laboratory 4455 Genesee Street Buffalo, N. Y. Attn: Dr. Gordon Hall	1
Dept. of Mechanical Engineering University of Delaware Newark, Delaware Attn: Dr. James P. Hartnett	1
AVCO Manufacturing Corp. Everett, Mass. Attn: Dr. Kantrowitz	1
General Electric Co. Missile and Space Vehicle Dept. 3198 Chestnut St. Philadelphia, Pa. Attn: Jerome Persh	1
Institute for Molecular Physics University of Maryland College Park, Maryland Attn: E. A. Mason	1

CATALOGING INFORMATION FOR LIBRARY USE

BIBLIOGRAPHIC INFORMATION

	DESCRIPTORS	CODES		DESCRIPTORS	CODES
SOURCE	NOL technical report	NOLTR	SECURITY CLASSIFICATION AND CODE COUNT	Unclassified - 14	UØ14
REPORT NUMBER	62 - 65	62ØØ65	CIRCULATION LIMITATION		
REPORT DATE	18 June 1962	Ø662	CIRCULATION LIMITATION OR BIBLIOGRAPHIC		
			BIBLIOGRAPHIC (SUPPL., VOL., ETC.)		

SUBJECT ANALYSIS OF REPORT

DESCRIPTORS	CODES	DESCRIPTORS	CODES	DESCRIPTORS	CODES
Nitric	NITC	Ballistics	BALS		
Oxide	OXID	Aeroballistics	AERB		
Gamma	GAMM				
Band	BAND				
Molecular	MOLC				
Rotational	ROTA				
Temperature	TEMP				
Experimental	EXPE				
Spectroscopy	SPES				
Absorption	ABSR				
Coefficients	COEF				
Constants	COSA				

Naval Ordnance Laboratory, White Oak, Md.
(NOL technical report 62-65)
UNRESOLVED FINE STRUCTURE OF THE NITRIC OXIDE GAMMA 0-0 BAND FOR THE DETERMINATION OF TEMPERATURE (U), by David Levine. 18 June 1962. 22p. illus., charts, tables. (Ballistics research report 63) UNCLASSIFIED

An experimental program was conducted to investigate the properties of the unresolved rotational fine structure of nitric oxide gamma 0-0 band. The experimental values were taken spectroscopically in absorption at controlled temperatures.

From the experimental absorption coefficients, temperatures were determined to within 6 percent of the directly measured values. The rotational constants of the upper and lower states could be determined to 13 percent and 6 percent, respectively, of the known values.

1. Nitric oxide - Properties
2. Nitric oxide - Temperatures
I. Title
II. Levine, David
III. Series

Abstract card is unclassified.

Naval Ordnance Laboratory, White Oak, Md.
(NOL technical report 62-65)
UNRESOLVED FINE STRUCTURE OF THE NITRIC OXIDE GAMMA 0-0 BAND FOR THE DETERMINATION OF TEMPERATURE (U), by David Levine. 18 June 1962. 22p. illus., charts, tables. (Ballistics research report 63) UNCLASSIFIED

An experimental program was conducted to investigate the properties of the unresolved rotational fine structure of nitric oxide gamma 0-0 band. The experimental values were taken spectroscopically in absorption at controlled temperatures.

From the experimental absorption coefficients, temperatures were determined to within 6 percent of the directly measured values. The rotational constants of the upper and lower states could be determined to 13 percent and 6 percent, respectively, of the known values.

1. Nitric oxide - Properties
2. Nitric oxide - Temperatures
I. Title
II. Levine, David
III. Series

Abstract card is unclassified.

Naval Ordnance Laboratory, White Oak, Md.
(NOL technical report 62-65)
UNRESOLVED FINE STRUCTURE OF THE NITRIC OXIDE GAMMA 0-0 BAND FOR THE DETERMINATION OF TEMPERATURE (U), by David Levine. 18 June 1962. 22p. illus., charts, tables. (Ballistics research report 63) UNCLASSIFIED

An experimental program was conducted to investigate the properties of the unresolved rotational fine structure of nitric oxide gamma 0-0 band. The experimental values were taken spectroscopically in absorption at controlled temperatures.

From the experimental absorption coefficients, temperatures were determined to within 6 percent of the directly measured values. The rotational constants of the upper and lower states could be determined to 13 percent and 6 percent, respectively, of the known values.

1. Nitric oxide - Properties
2. Nitric oxide - Temperatures
I. Title
II. Levine, David
III. Series

Abstract card is unclassified.

Naval Ordnance Laboratory, White Oak, Md.
(NOL technical report 62-65)
UNRESOLVED FINE STRUCTURE OF THE NITRIC OXIDE GAMMA 0-0 BAND FOR THE DETERMINATION OF TEMPERATURE (U), by David Levine. 18 June 1962. 22p. illus., charts, tables. (Ballistics research report 63) UNCLASSIFIED

An experimental program was conducted to investigate the properties of the unresolved rotational fine structure of nitric oxide gamma 0-0 band. The experimental values were taken spectroscopically in absorption at controlled temperatures.

From the experimental absorption coefficients, temperatures were determined to within 6 percent of the directly measured values. The rotational constants of the upper and lower states could be determined to 13 percent and 6 percent, respectively, of the known values.

1. Nitric oxide - Properties
2. Nitric oxide - Temperatures
I. Title
II. Levine, David
III. Series

Abstract card is unclassified.